

Comparison of the Galactic coordinate frames realized by the PPMXL and UCAC4 catalogues

V. V. Vityazev[★] and A. S. Tsvetkov

St Petersburg State University, 7/9 Universitetskaya nab., St Petersburg 199034, Russia

Accepted 2016 June 7. Received 2016 June 3; in original form 2016 April 24

ABSTRACT

We present a method of comparing the Galactic systems realized by two astrometric catalogues. The systematic differences between positions and proper motions are represented by vector spherical harmonics. To extract the signal from the noise, we use a statistical criterion adapted to using HEALPIX data pixelization to determine the significance of all the accessible harmonics. We also use a new analytical method that includes the magnitude equation in the vector spherical harmonics technique. The influence of the magnitude equation on the determination of the mutual orientation and rotation of the PPMXL and UCAC4 Galactic reference frames has been found in the range of J magnitudes from 10.25 to 15.75 mag. The angles of mutual orientation and the rates of mutual rotation of the Galactic frames under consideration depend on magnitude and can reach the level of 10 mas in orientation and 0.7 mas yr^{-1} for spin. We make a kinematic study of the low degree harmonics in the representation of the systematic differences between the Galactic proper motions. We have found that, averaged over the magnitude range, the biases of the Oort constants due to systematic differences of proper motions between the two catalogues, which are as large as $\langle \Delta A \rangle = 1.60 \pm 0.41$ and $\langle \Delta B \rangle = -1.91 \pm 0.32 \text{ km s}^{-1} \text{ kpc}^{-1}$, are greater than the standard errors of their evaluation in the systems of these catalogues. The theoretical equations used in this paper are based on real vector harmonics. We present a set of formulae to convert them into the complex function formalism.

Key words: catalogues – astrometry – reference systems – Galaxy: kinematics and dynamics.

1 INTRODUCTION

The pre-*Gaia* all-sky astrometric catalogues, PPMXL (Roeser, Demleitner & Schilbach 2010) and the Fourth United States Naval Observatory (USNO) CCD Astroglyph Catalogue (UCAC4; Zacharias et al. 2013), provide a basis for performing various astronomical studies. The PPMXL catalogue contains information about the International Celestial Reference System (ICRS) positions and proper motions of 900 million stars down to magnitude $V = 20$ with complete sky coverage. The mean errors of the proper motions lie within the range $4\text{--}10 \text{ mas yr}^{-1}$, while the positional accuracy at epoch 2000.0 is estimated to be $80\text{--}120 \text{ mas}$ for 410 million objects for which the positions in the Two-Micron All-Sky Survey (2MASS) catalogue (Skrutskie et al. 2006) are known. For the remaining stars, the positional accuracy varies between 150 and 300 mas.

The UCAC4 catalogue contains 113 million stars from magnitude 8 to 16 in a non-standard photometric band between V and R . It also

covers the entire sky. The positional accuracy at the mean epoch is estimated to be within the range $15\text{--}100 \text{ mas}$, while the formal errors of the proper motions are within the range $1\text{--}10 \text{ mas yr}^{-1}$. The systematic errors of the proper motions lie within the range $1\text{--}4 \text{ mas yr}^{-1}$. The catalogue was constructed in the ICRS and it is claimed that it is complete down to $R = 16$. The UCAC4 is the last catalogue in the UCAC project. No photographic observations were used in this project, because all measurements were made between 1998 and 2004 using CCD detectors only. At present, these catalogues are widely used in the visible as the optical ICRS reference frames for hundreds of millions of stars. According to the inner logics of astrometry, it is necessary to have the opportunity to pass from the system of one catalogue to the system of another catalogue. The authors of the UCAC4 catalogue (Zacharias et al. 2013) compared the proper motions of stars from the PPMXL and UCAC4 catalogues in a narrow right ascension (RA) zone from 6.0 to 6.1 h in the declination range from -60 to -30 deg . The HEALPIX (Gorski et al. 2005) partition of the sphere was used to table the differences PPMXL–UCAC4 (Farnocchia et al. 2015). Such an approach suggests using numerical interpolation to calculate the differences for a specific point on the sphere. In addition, the dependence of these differences on the magnitude of stars was disregarded in the presented data, and no

[★] E-mail: vityazev@list.ru

smoothing over the RA and Dec. was performed to reduce the random errors.

A proper solution of the problem of comparing catalogues suggests representing the systematic differences by the systems of orthogonal harmonics describing their dependence on the coordinates and magnitudes of stars (Bien et al. 1978; Mignard et al. 1990; Mignard 2000). With respect to the catalogues PPMXL and UCAC4, the first step in this direction was made by Vityazev & Tsvetkov (2015). In this paper, the comparison of the equatorial systems of these catalogues was done by representing the systematic differences by vector spherical harmonics (VSH). In contrast to previous similar works, we propose a new statistical criterion that allows us to estimate the significance of all the harmonics that can be calculated on the chosen HEALPIX pixelization scheme. Normalized Legendre polynomials were used to approximate the decomposition coefficients derived from groups of stars with different magnitudes. The constructed models of systematic differences were used to analyse the systematic differences as functions of three variables (α , δ , m).

The present paper complements these results with a comparison of the Galactic coordinate systems realized by the same catalogues. First, we describe the procedure to expand the individual differences on a set of real VSH and the Legendre polynomials. Then, we analyse the systematic differences of positions and proper motions in the Galactic systems in order to calculate the mutual orientation and spin of the frames under consideration. The last section of the paper is devoted to the kinematic interpretation of the systematic differences between the proper motions in the Galactic system. The theoretical equations used in this paper are based on real vector harmonics. In Appendices A and B, we give a list of equations for converting these results into expressions that would have occurred if the complex spherical harmonics were used.

2 DECOMPOSITION OF THE STELLAR VELOCITY FIELD ON VSH

Consider two orthogonal unit vectors \mathbf{e}_l and \mathbf{e}_b , respectively, in the directions of change in Galactic longitude and latitude in a plane tangential to the sphere. We introduce the following expression for the field of systematic stellar position differences:

$$\Delta \mathbf{F}(l, b) = \Delta l \cos b \mathbf{e}_l + \Delta b \mathbf{e}_b. \quad (1)$$

A similar expression is used to represent the systematic differences between the stellar proper motions.

Because the systematic differences between the positions and proper motions form a vector field, it is appropriate to use the technique of decomposing this field into a system of VSH. These functions were first used by Mignard et al. (1990) and Mignard (2000) for comparison of FK5 with *Hipparcos*. Here, the VSH were represented as the complex functions. A further development of this technique aimed at its application in the *Gaia* project was made by Mignard & Klioner (2012). In this paper, we use the VSH apparatus based on a representation of the spherical harmonics as the real functions. This formalism was used in our previous papers for a kinematic analysis of stellar proper motions (Vityazev & Tsvetkov 2013, 2014). Mathematical relations connecting both real and complex function approaches are shown in Appendices A and B.

In what follows, we use the decomposition of the field (1) in a system of VSH

$$\Delta \mathbf{F}(l, b) = \sum_{nkp} t_{nkp} \mathbf{T}_{nkp}(l, b) + \sum_{nkp} s_{nkp} \mathbf{S}_{nkp}(l, b), \quad (2)$$

where the toroidal \mathbf{T}_{nkp} and spheroidal \mathbf{S}_{nkp} functions are defined by equations (A10) and (A11). The decomposition coefficients t_{nkp} and s_{nkp} can be calculated from

$$t_{nkp} = \int_{\Omega} (\Delta \mathbf{F} \cdot \mathbf{T}_{nkp}) d\omega \quad (3)$$

and

$$s_{nkp} = \int_{\Omega} (\Delta \mathbf{F} \cdot \mathbf{S}_{nkp}) d\omega. \quad (4)$$

The calculation of the toroidal and spheroidal coefficients is the main goal in representing the systematic differences between the positions and proper motions of stars from two catalogues by VSH.

3 PRACTICAL IMPLEMENTATION FOR THE HEALPIX PARTITION OF THE SPHERE

When hundreds of millions of stars are compared, it is appropriate to use data pre-pixelization. We use the equal-area pixels constructed on the sphere according to the HEALPIX scheme (Gorski et al. 2005). In this scheme, the number N_{side} is the key parameter (resolution parameter) defining the partition of the sphere into equal pixels. The total number of pixels is $N = 12N_{\text{side}}^2$. The entire sphere is divided by two parallels with declinations $\pm \arcsin(2/3)$ into three parts, the equatorial and two polar ones. In each of the polar zones, $N_{\text{side}} - 1$ parallels is chosen; the number of parallels in the equatorial zone is $(2N_{\text{side}} + 1)$. The centres of $4N_{\text{side}}$ pixels lie on each parallel of the equatorial region. The two parallels closest to the poles always contain four pixels, while the number of pixels on each parallel increases by one when moving from the poles to the equator in the polar zones. The pixels are numbered $q = 0, \dots, N - 1$ along the parallels from north to south

To calculate the coefficients of the VSH decomposition of the systematic differences, we now have the following formulae instead of equations (3) and (4):

$$t_{nkp} = \frac{4\pi}{N} \sum_{q=0}^{N-1} \Delta \mathbf{F}(l_q, b_q) \mathbf{T}_{nkp}(l_q, b_q); \quad (5)$$

$$s_{nkp} = \frac{4\pi}{N} \sum_{q=0}^{N-1} \Delta \mathbf{F}(l_q, b_q) \mathbf{S}_{nkp}(l_q, b_q). \quad (6)$$

Here, $\Delta \mathbf{F}(l_q, b_q)$ is the mean value of the field in the q th pixel referred to its centre.

3.1 Significant terms in the VSH decomposition of systematic differences

To detect the significant terms of the decomposition, we propose a method that allows the signal components of the decomposition to be detected with a specified probability among all the admissible indices k and n for the pixelization scheme used. This done, the numerical values of the significant decomposition coefficients are immediately determined from a single application of the least-squares method (LSM). This approach is analogous to the spectral analysis of evenly spaced time series, where the significance of the periodogram peaks is determined for all its peaks in the frequency range admissible by the sampling rate. In our case, the squares of the coefficients t_{nkp} and s_{nkp} can be considered as the periodogram values, and the determination of their significance is based on the fact that the coefficients s_{nkp} and t_{nkp} for normally distributed centred

noise with variance $\sigma_0^2 = 1$ are normally distributed random variables with zero mean and unit variance. Consequently, the squares of the amplitudes s_{nkp}^2 and t_{nkp}^2 are random variables distributed according to the chi-square law with one degree of freedom. The limiting value of index k must be taken as $k_{\max} = 4N_{\text{side}} - 1$ to avoid the aliasing effects. Therefore, the harmonics should be checked in index k for $k = 0, \dots, k_{\max}$. The limiting value of our series $n = k, \dots, n_{\max}$, for each admissible index k is determined from the condition that an adopted accuracy of calculating the squares of the norms of the basis functions breaks down. For further details, the reader is referred to Vityazev & Tsvetkov (2015).

3.2 Magnitude equation

In astrometric catalogues, the dependence of systematic differences on the magnitude of stars in a particular photometric band is traditionally called the magnitude equation. To take this into account, we can represent the vector field in the form

$$\Delta \mathbf{F}(l, b, m) = \sum_{nkp} t_{nkp}(m) \mathbf{T}_{nkp}(l, b) + \sum_{nkp} s_{nkp}(m) \mathbf{S}_{nkp}(l, b), \quad (7)$$

where the coefficients $t_{nkp}(m)$ and $s_{nkp}(m)$ are functions of the magnitude. These coefficients are approximated using appropriate polynomials $Q_r(m)$ by expressions of the form

$$t_{nkp}(m) = \sum_r t_{nkpr} Q_r(m) \quad (8)$$

and

$$s_{nkp}(m) = \sum_r s_{nkpr} Q_r(m). \quad (9)$$

Substituting equation (8) into equation (7) gives the final form of the model of systematic differences:

$$\Delta \mathbf{F}(l, b, m) = \sum_{nkpr} t_{nkpr} \mathbf{T}_{nkp}(l, b) Q_r(m) + \sum_{nkpr} s_{nkpr} \mathbf{S}_{nkp}(l, b) Q_r(m). \quad (10)$$

Obviously, the following procedure can be proposed to consider the magnitude equation when the systematic differences are approximated by orthogonal functions. In this method, the coefficients $t_{nkp}(m)$ and $s_{nkp}(m)$ are obtained from the stars belonging to small magnitude bins, and then the derived decomposition coefficients referred to the mean values of the magnitude bins are approximated by expressions (8) and (9). This approach is possible if all-sky catalogues are available, when samples containing a sufficiently large number of stars with approximately the same magnitude can be produced. This approach was used for the first time in Vityazev & Tsvetkov (2015).

4 APPLICATION TO THE CATALOGUES PPMXL AND UCAC4

In our work, we obtained systematic differences between the PPMXL and UCAC4 catalogues as functions of coordinates and magnitude in three steps.

In the first step, we partitioned the sphere by the HEALPIX method into 1200 pixels with an area of 34.4 deg^2 . Using the star identification procedure in the J band (2MASS photometric system), we compiled a list of 41 316 676 stars belonging to the PPMXL,

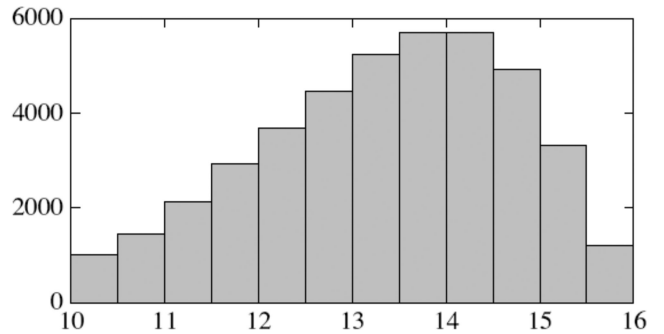


Figure 1. Magnitude distribution of stars from the sample of 41 316 676 stars. The J magnitudes and the number of stars (in thousands) are along the horizontal and vertical axes, respectively.

UCAC4 and XPM catalogues (Fedorov, Myznikov & Akhmetov 2009). The distribution of stars in magnitudes is shown in Fig. 1 taken from (Vityazev & Tsvetkov 2015). Because of the identification procedure, all the unrealistic outliers, greater than 500 mas, either in $\Delta\alpha\cos\delta$ or $\Delta\delta$, were not allowed for straight averaging in each pixel. After averaging the differences between the stellar positions and proper motions over the pixels, we formed the differences PPMXL–UCAC4 between the stellar positions and proper motions in the Galactic coordinate system referred to the centres of our pixels. These data were generated for 12 0.5-mag bins from 10.25 to 15.75 mag. On average, there were up to 1000 stars for each pixel and each magnitude bin; therefore, the noise level in the averaged differences decreased approximately by a factor of 30 compared to that in the initial differences. From this point of view, the catalogues of mean differences can be considered as the tables of m -dependent systematic differences at fixed points. The systematic differences for any point on the sphere and any magnitude can be obtained by interpolation. Note that such a representation of systematic differences was used by Mignard (2000) and Farnocchia et al. (2015).

In the second step, the tabular differences were approximated by VSH in accordance with equation (7). The coefficients $t_{nkp}(m)$ and $s_{nkp}(m)$ in this equation were obtained for each mean magnitude of the samples of stars used. The algorithm for the VSH decomposition of the systematic differences consists of the following points.

Point 1. We determine the indices of the statistically significant harmonics. This procedure consisted of checking conditions that correspond to the detection of harmonics with a probability of 0.99 according to the chi-square test. For our pixelization scheme, the limiting value of the index k is $k = 39$, while the highest values of the indices n were determined from the condition that the error of calculating the squares of the norms of the basis functions exceeds 1 percent.

Point 2. We determine the numerical values of the coefficients $t_{nkp}(m_i)$ and $s_{nkp}(m_i)$ and their rms errors $\bar{t}_{nkp}(m_i)$ and $\bar{s}_{nkp}(m_i)$ by the LSM from the set of statistically significant harmonics selected in Step 1.

In the third step, the coefficients $t_{nkp}(m_i)$ and $s_{nkp}(m_i)$ are approximated by normalized Legendre polynomials,

$$t_{nkp}(m) = \sum_r t_{nkpr} Q_r(\bar{m}) \quad (11)$$

and

$$s_{nkp}(m) = \sum_r s_{nkpr} Q_r(\bar{m}), \quad (12)$$

where

$$Q_r(\bar{m}) = \sqrt{\frac{2r+1}{2}} P_r(\bar{m}), \quad (13)$$

and $P_r(\bar{m})$ are Legendre polynomials. The following recurrence relation can be used to calculate the latter:

$$P_{r+1}(\bar{m}) = \frac{2r+1}{r+1} \bar{m} P_r(\bar{m}) - \frac{r}{r+1} P_{r-1}(\bar{m}),$$

$$r = 1, 2, \dots, \quad P_0 = 1, \quad P_1 = \bar{m}. \quad (14)$$

If $m_{\min} \leq m \leq m_{\max}$, then the argument of the Legendre polynomials belonging to the closed interval $[-1; +1]$ is calculated from

$$\bar{m} = 2 \frac{m - m_{\min}}{m_{\max} - m_{\min}} - 1. \quad (15)$$

In theory, the degree of fitted polynomial r should not be larger than the number of equations of condition minus one. We have established the statistically significant harmonics in index r by taking into account the fact that the same toroidal or spheroidal coefficient with a set of indices $nkpr$ could be significant according to the chi-square test for one J sample, and insignificant for another. For this reason, the magnitude equation was determined only for those coefficients that turned out to be significant at least in three magnitude samples. In this case, the values for such a coefficient were determined for all 12 J samples. Otherwise, the harmonic was rejected. Further, the coefficients t_{nkpr} and s_{nkpr} were derived by the LSM solutions of equations (31) and (12) written for all 12 magnitudes. The degree of the approximating polynomial is taken to be three as all upper ones turned out to be insignificant. In addition, in order that the rms errors of the sought for coefficients reflect the accuracy of the initial coefficients $t_{nkpr}(m)$ and $s_{nkpr}(m)$ rather than the accuracy of the formal approximation of the curves $t = t_{nkpr}(m)$ and $s = s_{nkpr}(m)$, the rms errors of the approximation coefficients t_{nkpr} and s_{nkpr} were calculated from

$$\sigma(t_{nkpr}) = \sqrt{\sum_{q=0}^3 w_{rq}^2 \sum_{i=0}^{11} Q_r^2(\bar{m}_i) \bar{t}_{nkpr}^2(m_i)} \quad (16)$$

and

$$\sigma(s_{nkpr}) = \sqrt{\sum_{q=0}^3 w_{rq}^2 \sum_{i=0}^{11} Q_r^2(\bar{m}_i) \bar{s}_{nkpr}^2(m_i)}. \quad (17)$$

Here, w_{rq} denote the elements of the inverse matrices of the normal systems of equations corresponding to the LSM solution of equations (31) and (12), while $\bar{t}_j(m_i)$ and $\bar{s}_j(m_i)$ denote the rms errors of the coefficients $t_{nkpr}(m_i)$ and $s_{nkpr}(m_i)$ found in the point 2 of the second step. The final toroidal and spheroidal decomposition coefficients t_{nkpr} and s_{nkpr} of the systematic differences between the PPMXL and UCAC4 stellar positions and proper motions in the Galactic coordinate systems are given in Tables 1–4.

5 MAGNITUDE EQUATION IN THE VISIBLE RANGE

Here, some remarks should be made concerning the choice of the photometric band for magnitude equation. Because PPMXL and UCAC4 are optical catalogues, the B , V and R magnitudes are appropriate, of which only B and R are common for both catalogues. However, the B and R magnitudes are taken from different sources so one and the same star in both catalogues is attributed to different B magnitudes as well as to different R magnitudes. This creates at least two problems. The first problem arises in the process of the cross-identification of stars, and the second problem arises in deriving

Table 1. Toroidal decomposition coefficients t_{nkpr} of the field of stellar position differences PPMXL–UCAC4 $\Delta l \cos b e_l + \Delta b e_b$ with the index r due to the magnitude equation. The units of measurement are mas.

t_{nkpr}		t_{nkpr}	
$t_{1,0,1,0}$	-12.77 ± 0.33	$t_{4,1,1,0}$	4.01 ± 0.33
$t_{1,0,1,1}$	-4.26 ± 0.41	$t_{4,3,1,0}$	3.34 ± 0.33
$t_{1,1,0,0}$	-5.47 ± 0.35	$t_{4,4,0,0}$	2.72 ± 0.33
$t_{1,1,0,1}$	-7.22 ± 0.41	$t_{5,0,1,0}$	-1.78 ± 0.35
$t_{1,1,0,2}$	-2.07 ± 0.44	$t_{5,0,1,1}$	0.96 ± 0.41
$t_{1,1,1,0}$	8.47 ± 0.35	$t_{5,0,1,2}$	1.18 ± 0.44
$t_{1,1,1,1}$	5.48 ± 0.41	$t_{5,1,0,0}$	1.85 ± 0.34
$t_{1,1,1,2}$	2.08 ± 0.44	$t_{5,1,0,1}$	1.22 ± 0.42
$t_{2,0,1,0}$	-1.43 ± 0.33	$t_{5,1,1,0}$	-1.93 ± 0.34
$t_{2,0,1,1}$	1.23 ± 0.41	$t_{5,2,0,0}$	-1.46 ± 0.37
$t_{2,1,0,0}$	1.01 ± 0.35	$t_{5,4,0,0}$	-5.06 ± 0.33
$t_{2,1,0,1}$	-7.35 ± 0.49	$t_{5,4,0,1}$	-2.13 ± 0.41
$t_{2,1,0,2}$	-6.50 ± 0.44	$t_{5,5,0,0}$	2.51 ± 0.33
$t_{2,1,0,3}$	-3.37 ± 0.47	$t_{6,0,1,0}$	-1.88 ± 0.33
$t_{2,1,1,0}$	-2.55 ± 0.33	$t_{6,2,0,0}$	-1.95 ± 0.34
$t_{2,1,1,1}$	4.10 ± 0.41	$t_{6,4,0,0}$	-2.11 ± 0.33
$t_{2,2,0,1}$	5.61 ± 0.49	$t_{6,5,0,0}$	3.71 ± 0.33
$t_{2,2,0,2}$	4.20 ± 0.43	$t_{6,5,0,1}$	1.35 ± 0.41
$t_{2,2,0,3}$	2.23 ± 0.47	$t_{6,5,1,0}$	2.68 ± 0.35
$t_{2,2,1,0}$	-1.02 ± 0.35	$t_{6,5,1,1}$	1.57 ± 0.41
$t_{2,2,1,1}$	2.84 ± 0.49	$t_{6,5,1,2}$	1.04 ± 0.44
$t_{2,2,1,2}$	1.55 ± 0.44	$t_{6,6,1,0}$	-3.69 ± 0.33
$t_{2,2,1,3}$	1.84 ± 0.47	$t_{7,0,1,0}$	1.00 ± 0.33
$t_{3,2,1,0}$	-2.34 ± 0.33	$t_{7,0,1,1}$	-0.75 ± 0.41
$t_{3,2,1,1}$	-1.70 ± 0.41	$t_{10,9,1,0}$	2.40 ± 0.33
$t_{3,3,0,1}$	-0.89 ± 0.41	$t_{45,39,0,0}$	-1.86 ± 0.33
$t_{4,1,0,0}$	-3.46 ± 0.35	$t_{53,39,1,0}$	1.72 ± 0.33
$t_{4,1,0,1}$	2.54 ± 0.49	$t_{53,39,1,1}$	1.49 ± 0.41
$t_{4,1,0,2}$	1.65 ± 0.44	$t_{55,39,0,0}$	-2.49 ± 0.38
$t_{4,1,0,3}$	1.16 ± 0.47	$t_{55,39,1,0}$	-1.89 ± 0.39

the magnitude equation. Fortunately, many stars in PPMXL and UCAC4 are supplemented with the near-infrared photometry in the J , H and K_s bands borrowed from the 2MASS. This makes it possible to use each of them, in particular the J band, for cross-identification and for derivation of the magnitude equation. As mentioned in the previous section, the J magnitude equation was constructed with the coefficients given in Tables 1–4. To adjust this magnitude equation to any other photometric band, it is necessary to know the conversion formulae to pass from a chosen band to the J band. With this aim, we found the mean values of B and R magnitudes and their standard deviations for all the stars for which the B , R and J colours are available. This was done in each 0.1-mag width J band with mean magnitudes from $J = 10$ to $J = 16$. After smoothing these values with the five-point moving average filter, the resulting magnitudes with 0.5-mag intervals were fitted with linear functions, which can be used to connect B and R with the J magnitude, and vice versa. For the PPMXL catalogue, these relations turned out to be:

$$B = (0.767 \pm 0.008)J + (6.466 \pm 0.111), \quad 10.25 \leq J \leq 15.75; \quad (18)$$

$$J = (1.304 \pm 0.014)B - (8.433 \pm 0.171), \quad 14.33 \leq B \leq 18.55; \quad (19)$$

$$R = (0.823 \pm 0.009)J + (4.372 \pm 0.116), \quad 10.25 \leq J \leq 15.75; \quad (20)$$

Table 2. Spheroidal decomposition coefficients s_{nkpr} of the field of stellar position differences PPMXL–UCAC4 $\Delta l \cos b e_l + \Delta b e_b$ with the index r due to the magnitude equation. The units of measurement are mas.

s_{nkpr}	s_{nkpr}	s_{nkpr}	s_{nkpr}
$s_{1,0,1,1}$	2.70 ± 0.49	$s_{3,2,0,0}$	-5.32 ± 0.33
$s_{1,0,1,2}$	1.68 ± 0.42	$s_{3,2,0,1}$	1.89 ± 0.49
$s_{1,0,1,3}$	3.06 ± 0.47	$s_{3,2,0,3}$	-1.12 ± 0.47
$s_{1,1,0,0}$	1.04 ± 0.35	$s_{3,2,1,0}$	-2.96 ± 0.33
$s_{1,1,0,1}$	3.51 ± 0.49	$s_{3,3,1,0}$	5.87 ± 0.33
$s_{1,1,0,2}$	1.68 ± 0.44	$s_{3,3,1,3}$	1.24 ± 0.41
$s_{1,1,0,3}$	2.39 ± 0.47	$s_{4,1,1,0}$	4.28 ± 0.35
$s_{1,1,1,0}$	-7.68 ± 0.35	$s_{4,1,1,2}$	1.40 ± 0.44
$s_{1,1,1,1}$	-5.17 ± 0.49	$s_{4,2,0,0}$	1.45 ± 0.33
$s_{1,1,1,2}$	-4.59 ± 0.44	$s_{4,2,0,3}$	1.00 ± 0.41
$s_{1,1,1,3}$	-2.67 ± 0.47	$s_{4,4,1,0}$	2.29 ± 0.33
$s_{2,1,0,0}$	1.80 ± 0.33	$s_{5,0,1,0}$	-1.57 ± 0.33
$s_{2,1,0,1}$	2.96 ± 0.41	$s_{5,0,1,1}$	1.52 ± 0.41
$s_{2,1,1,0}$	-4.86 ± 0.33	$s_{5,2,1,0}$	1.45 ± 0.36
$s_{2,1,1,1}$	-2.75 ± 0.41	$s_{6,1,1,0}$	-3.05 ± 0.34
$s_{2,2,0,0}$	-2.56 ± 0.35	$s_{6,5,1,0}$	-2.18 ± 0.33
$s_{2,2,0,1}$	-3.35 ± 0.41	$s_{6,5,1,1}$	-2.38 ± 0.41
$s_{2,2,0,2}$	1.32 ± 0.44	$s_{6,6,1,0}$	1.83 ± 0.33
$s_{2,2,1,0}$	-5.02 ± 0.35	$s_{6,6,1,1}$	2.35 ± 0.41
$s_{2,2,1,1}$	-1.55 ± 0.41	$s_{7,0,1,0}$	2.01 ± 0.33
$s_{2,2,1,2}$	2.05 ± 0.44	$s_{9,0,1,0}$	-2.45 ± 0.33
$s_{3,0,1,1}$	1.14 ± 0.41	$s_{9,7,0,0}$	1.42 ± 0.33
$s_{3,0,1,2}$	3.06 ± 0.42	$s_{10,8,0,0}$	-1.11 ± 0.33
$s_{3,1,0,0}$	-1.20 ± 0.35	$s_{10,8,0,1}$	-2.72 ± 0.41
$s_{3,1,0,1}$	-0.97 ± 0.41	$s_{11,0,1,0}$	1.93 ± 0.33
$s_{3,1,0,2}$	1.96 ± 0.44		

Table 3. Toroidal decomposition coefficients t_{nkpr} of the field of stellar proper motions differences PPMXL–UCAC4 $\Delta \mu_l \cos b e_l + \Delta \mu_b e_b$ with the index r due to the magnitude equation. The units of measurement are mas yr⁻¹.

t_{nkpr}	t_{nkpr}	t_{nkpr}	t_{nkpr}
$t_{1,0,1,0}$	-1.68 ± 0.05	$t_{3,1,0,2}$	0.13 ± 0.05
$t_{1,0,1,2}$	0.18 ± 0.05	$t_{3,2,0,1}$	0.57 ± 0.05
$t_{1,0,1,3}$	0.13 ± 0.04	$t_{3,2,0,2}$	0.08 ± 0.04
$t_{1,1,0,0}$	-1.07 ± 0.05	$t_{3,2,1,0}$	0.84 ± 0.05
$t_{1,1,0,1}$	-0.36 ± 0.05	$t_{3,2,1,1}$	0.30 ± 0.05
$t_{1,1,0,2}$	0.59 ± 0.05	$t_{3,3,0,0}$	0.51 ± 0.05
$t_{1,1,1,2}$	-0.41 ± 0.04	$t_{3,3,0,2}$	-0.11 ± 0.05
$t_{2,1,0,0}$	-1.61 ± 0.05	$t_{3,3,1,0}$	-1.07 ± 0.05
$t_{2,1,0,1}$	-0.63 ± 0.05	$t_{3,3,1,1}$	-0.43 ± 0.05
$t_{2,1,0,2}$	0.30 ± 0.05	$t_{4,1,1,0}$	0.35 ± 0.05
$t_{2,1,0,3}$	-0.20 ± 0.05	$t_{4,1,1,1}$	0.38 ± 0.05
$t_{2,1,1,0}$	0.43 ± 0.05	$t_{4,3,1,0}$	0.20 ± 0.05
$t_{2,1,1,1}$	-0.15 ± 0.05	$t_{4,3,1,1}$	0.47 ± 0.05
$t_{2,1,1,2}$	-0.34 ± 0.05	$t_{4,3,1,3}$	-0.10 ± 0.05
$t_{2,1,1,3}$	0.17 ± 0.05	$t_{4,4,0,0}$	0.66 ± 0.05
$t_{2,2,0,0}$	2.97 ± 0.05	$t_{4,4,0,1}$	0.11 ± 0.05
$t_{2,2,0,1}$	0.53 ± 0.05	$t_{5,0,1,0}$	-0.68 ± 0.05
$t_{2,2,0,2}$	-0.34 ± 0.05	$t_{5,1,0,0}$	0.71 ± 0.06
$t_{2,2,0,3}$	0.16 ± 0.05	$t_{5,1,0,1}$	0.24 ± 0.05
$t_{2,2,1,0}$	0.80 ± 0.05	$t_{6,5,1,0}$	0.61 ± 0.05
$t_{2,2,1,1}$	0.28 ± 0.05	$t_{6,5,1,1}$	0.10 ± 0.05
$t_{2,2,1,2}$	-0.22 ± 0.05	$t_{7,6,1,0}$	0.37 ± 0.05
$t_{3,0,1,0}$	0.84 ± 0.05	$t_{9,3,1,0}$	0.49 ± 0.05
$t_{3,0,1,1}$	0.43 ± 0.05	$t_{13,5,0,0}$	0.53 ± 0.05
$t_{3,0,1,2}$	0.10 ± 0.05	$t_{13,5,0,2}$	-0.09 ± 0.05
$t_{3,1,0,0}$	-0.49 ± 0.05	$t_{49,31,0,0}$	0.43 ± 0.05
$t_{3,1,0,1}$	-0.20 ± 0.05		

Table 4. Spheroidal decomposition coefficients s_{nkpr} of the field of stellar proper motions differences PPMXL–UCAC4 $\Delta \mu_l \cos b e_l + \Delta \mu_b e_b$ with the index r due to the magnitude equation. The units of measurement are mas yr⁻¹.

s_{nkpr}	s_{nkpr}	s_{nkpr}	s_{nkpr}
$s_{1,0,1,0}$	-2.31 ± 0.05	$s_{3,2,0,3}$	-0.11 ± 0.05
$s_{1,0,1,1}$	-0.56 ± 0.05	$s_{3,2,1,0}$	-0.46 ± 0.05
$s_{1,0,1,2}$	-0.25 ± 0.05	$s_{3,2,1,1}$	0.40 ± 0.05
$s_{1,1,0,0}$	-4.46 ± 0.05	$s_{3,2,1,3}$	-0.14 ± 0.05
$s_{1,1,0,1}$	-0.91 ± 0.05	$s_{3,3,1,0}$	0.64 ± 0.05
$s_{1,1,0,2}$	-0.37 ± 0.05	$s_{3,3,1,3}$	0.11 ± 0.04
$s_{1,1,0,3}$	0.10 ± 0.05	$s_{4,0,1,0}$	-0.48 ± 0.05
$s_{1,1,1,0}$	-1.06 ± 0.05	$s_{4,0,1,1}$	-0.26 ± 0.05
$s_{1,1,1,1}$	0.45 ± 0.05	$s_{4,1,1,0}$	0.98 ± 0.05
$s_{1,1,1,2}$	0.31 ± 0.05	$s_{4,1,1,1}$	0.19 ± 0.05
$s_{1,1,1,3}$	-0.26 ± 0.05	$s_{4,1,1,2}$	-0.23 ± 0.05
$s_{2,0,1,0}$	0.55 ± 0.05	$s_{5,2,1,0}$	0.47 ± 0.05
$s_{2,0,1,1}$	0.12 ± 0.05	$s_{5,3,0,0}$	0.46 ± 0.05
$s_{2,0,1,2}$	-0.09 ± 0.05	$s_{5,3,0,1}$	0.14 ± 0.05
$s_{2,1,0,0}$	-1.60 ± 0.05	$s_{6,0,1,0}$	-0.59 ± 0.05
$s_{2,1,0,1}$	-0.32 ± 0.05	$s_{6,2,0,0}$	-0.42 ± 0.05
$s_{2,1,0,2}$	0.24 ± 0.05	$s_{6,2,0,1}$	0.12 ± 0.05
$s_{2,1,0,3}$	-0.14 ± 0.05	$s_{6,2,1,0}$	-0.74 ± 0.06
$s_{2,1,1,0}$	-0.92 ± 0.05	$s_{6,2,1,2}$	0.12 ± 0.06
$s_{2,1,1,2}$	0.13 ± 0.05	$s_{6,3,0,0}$	0.85 ± 0.05
$s_{2,2,0,0}$	1.07 ± 0.05	$s_{6,3,0,1}$	0.15 ± 0.05
$s_{2,2,0,1}$	0.25 ± 0.05	$s_{6,3,0,2}$	-0.10 ± 0.05
$s_{2,2,1,0}$	1.11 ± 0.05	$s_{6,4,0,0}$	-0.51 ± 0.05
$s_{2,2,1,1}$	0.59 ± 0.05	$s_{6,4,0,1}$	0.16 ± 0.05
$s_{2,2,1,2}$	-0.15 ± 0.05	$s_{6,5,0,0}$	0.34 ± 0.05
$s_{3,0,1,1}$	0.33 ± 0.05	$s_{6,5,0,1}$	-0.15 ± 0.05
$s_{3,0,1,2}$	0.24 ± 0.04	$s_{7,0,1,0}$	-0.31 ± 0.05
$s_{3,0,1,3}$	-0.14 ± 0.05	$s_{7,0,1,1}$	-0.23 ± 0.05
$s_{3,1,0,0}$	-0.43 ± 0.05	$s_{7,0,1,2}$	0.10 ± 0.05
$s_{3,1,0,2}$	0.13 ± 0.05	$s_{7,2,1,0}$	-0.61 ± 0.05
$s_{3,2,0,0}$	-0.52 ± 0.05	$s_{7,2,1,1}$	-0.14 ± 0.05
$s_{3,2,0,1}$	-0.23 ± 0.05	$s_{8,7,0,0}$	-0.54 ± 0.05
$s_{3,2,0,2}$	0.09 ± 0.05	$s_{10,10,0,0}$	0.59 ± 0.05

$$J = (1.215 \pm 0.013)R - (5.310 \pm 0.152), \quad 12.81 \leq R \leq 17.33. \quad (21)$$

For the UCAC4 catalogue, they are:

$$B = (0.726 \pm 0.015)J + (6.300 \pm 0.190), \quad 10.25 \leq J \leq 15.75; \quad (22)$$

$$J = (1.378 \pm 0.028)B - (8.680 \pm 0.316), \quad 13.74 \leq B \leq 17.74; \quad (23)$$

$$R = (0.833 \pm 0.011)J + (3.725 \pm 0.144), \quad 10.25 \leq J \leq 15.75; \quad (24)$$

$$J = (1.200 \pm 0.016)R - (4.471 \pm 0.183), \quad 12.26 \leq R \leq 16.85. \quad (25)$$

Thus, to obtain the magnitude equation in PPMXL for stars with B or R magnitude, we should calculate the corresponding J magnitudes from equations (19) and (21) and substitute them into equation (15). For the UCAC4 catalogue, the J magnitudes are derived from equations (23) and (25).

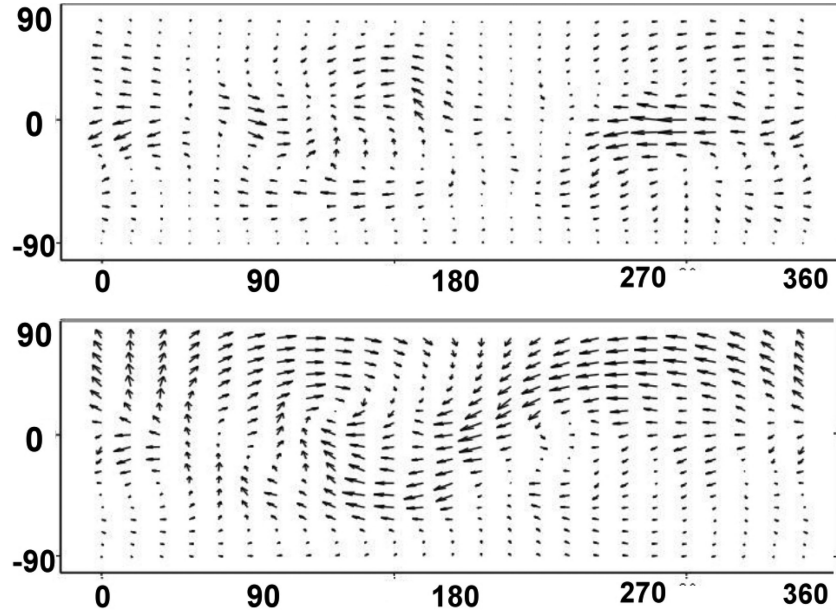


Figure 2. Vector fields $\Delta l \cos b \mathbf{e}_l + \Delta b \mathbf{e}_b$ for $J = 12$ (upper panel) and $J = 15$ (lower panel). The longitudes (deg) and latitudes (deg) are along the horizontal and vertical axes, respectively.

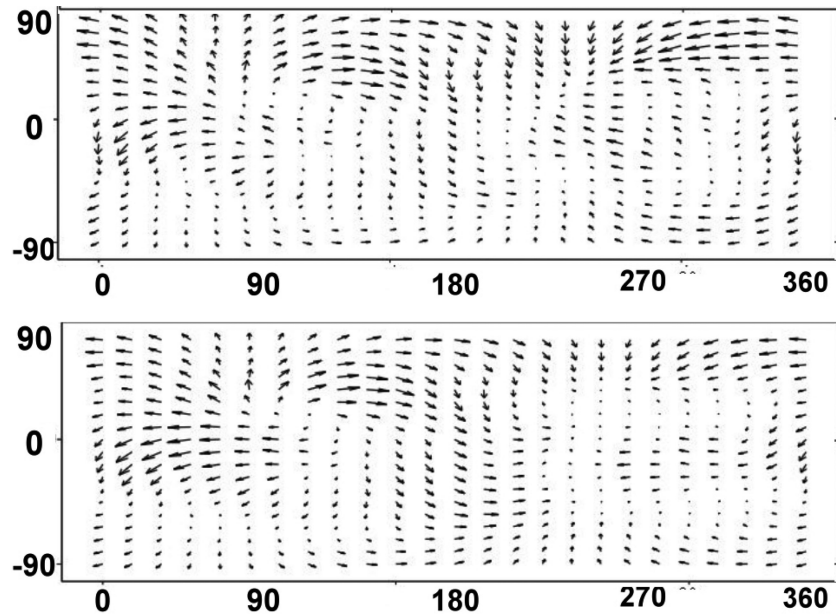


Figure 3. Vector fields $\Delta \mu_l \cos b \mathbf{e}_l + \Delta \mu_b \mathbf{e}_b$ for $J = 12$ (upper panel) and $J = 15$ (lower panel). The longitudes (deg) and latitudes (deg) are along the horizontal and vertical axes, respectively.

6 ANALYSIS OF THE GALACTIC SYSTEMATIC DIFFERENCES

Using toroidal and spheroidal coefficients from Tables 1–4, we can calculate the vector plots on the celestial sphere showing the fields of systematic differences of positions and proper motions. The results for bright ($J = 12$) and faint ($J = 15$) stars are shown in Figs 2 and 3. These plots correspond to all significant harmonics found. Now, we are going to use the first-order harmonics to see how close the principal Galactic axes of each catalogues are, and to see how different the kinematic parameters derived from proper motions of the catalogues under consideration can be.

Denote by $\epsilon_x, \epsilon_y, \epsilon_z$ the angles to rotate the system UCAC4 to ensure it coincides with the system PPMXL. With these notations, the systematic differences are modelled as

$$\Delta l \cos b = \epsilon_x \sin b \cos l + \epsilon_y \sin b \sin l - \epsilon_z \cos b, \quad (26)$$

and

$$\Delta b = -\epsilon_x \sin l + \epsilon_y \cos l. \quad (27)$$

The systematic differences between the positions and proper motions of the same stars reveal the differences between the reference frames that are realized by the catalogues under consideration. Froeschle et al. (1982) have shown that the rotation angles of the coordinate systems and the rates of their change can be determined

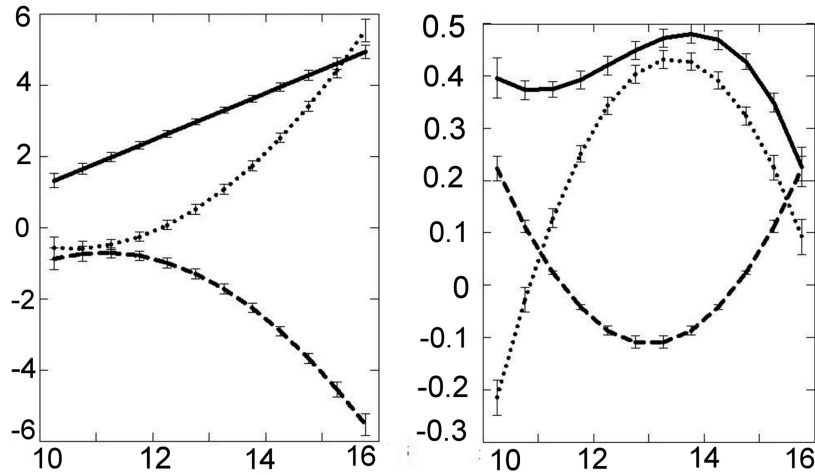


Figure 4. The left panel shows rotation angles (mas) to bring the UCAC4 Galactic frame into coincidence with the PPMXL frame: ϵ_x (dashes), ϵ_y (dots) and ϵ_z (solid line). The right panel shows the rates of the corresponding rotation angles (in mas yr⁻¹): ω_x (dashes), ω_y (dots) and ω_z (solid line). The J magnitudes of the samples are along the horizontal axes.

by analysing the systematic differences between the positions and proper motions. The same effects also manifest themselves in the coefficients of the decomposition of the systematic stellar position and proper motion differences into orthogonal functions. Within the model of solid-body rotation, the relationship between the rotation angles of one coordinate system relative to another and the coefficients of the decomposition of the systematic differences between the RA and Dec. of stars into scalar harmonics was established by Vityazev (1989, 1993). When using VSH, such a relationship was found by Mignard et al. (1990), who showed that the first-order toroidal coefficients in the decomposition of the systematic position differences define the mutual orientation of the reference frames associated with the catalogues under study, while the same coefficients in the decomposition of the systematic stellar proper motion differences allow the rate of mutual rotation of these frames to be calculated. In our case, the working formulae establishing the relationships between the rotation components and the first-order toroidal coefficients can be obtained for each magnitude by simple expansions of equations (26) and (27) into the VSH:

$$\epsilon_x(m) = -t_{1,1,1}(m)/2.89; \quad (28)$$

$$\epsilon_y(m) = -t_{1,1,0}(m)/2.89; \quad (29)$$

$$\epsilon_z(m) = -t_{1,0,1}(m)/2.89. \quad (30)$$

Here, with t_{nkpr} taken from Table 1, we have

$$t_{nkpr}(m) = \sum_r t_{nkpr} Q_r(\vec{m}). \quad (31)$$

Obviously, the angles ϵ_x , ϵ_y , ϵ_z allow the coordinates of the pole of the mutual rotation axis on the celestial sphere to be determined as

$$A_{\text{rot}} = \arctg\left(\frac{\epsilon_y}{\epsilon_x}\right), \quad D_{\text{rot}} = \arctg\left(\frac{\epsilon_z}{\sqrt{\epsilon_x^2 + \epsilon_y^2}}\right). \quad (32)$$

Beside this, an angle of mutual rotation around the rotation pole is derived from

$$\Delta\Omega_{\text{rot}}(m) = \sqrt{\epsilon_x^2(m) + \epsilon_y^2(m) + \epsilon_z^2(m)}. \quad (33)$$

In the same way, with notations ω_x , ω_y , ω_z for the rates of the PPMXL rotation in the UCAC4, the systematic differences in the proper motions are

$$\Delta\mu_l \cos b = \omega_x \sin b \cos l + \omega_y \sin b \sin l - \omega_z \cos b \quad (34)$$

and

$$\Delta\mu_b = -\omega_x \sin l + \omega_y \cos l. \quad (35)$$

Again, the working formulae establishing the relationships between the rates of rotation and the corresponding first-order toroidal coefficients can be obtained for each magnitude by simple expansions of equations (34) and (35) into the VSH:

$$\omega_x(m) = -t_{1,1,1}(m)/2.89; \quad (36)$$

$$\omega_y(m) = -t_{1,1,0}(m)/2.89; \quad (37)$$

$$\omega_z(m) = -t_{1,0,1}(m)/2.89. \quad (38)$$

Here, the values $t_{nkpr}(m)$ are calculated from equation (31) with appropriate coefficients t_{nkpr} , taken this time from Table 3. In turn, the rates ω_x , ω_y , ω_z define the coordinates of the pole of the spin

$$A_{\text{spin}} = \arctg\left(\frac{\omega_y}{\omega_x}\right), \quad D_{\text{spin}} = \arctg\left(\frac{\omega_z}{\sqrt{\omega_x^2 + \omega_y^2}}\right), \quad (39)$$

and the full angular velocity around this pole

$$\Delta\Omega_{\text{spin}}(m) = \sqrt{\omega_x^2(m) + \omega_y^2(m) + \omega_z^2(m)}. \quad (40)$$

Fig. 4 shows the dependence of rotation parameters to bring the UCAC4 Galactic frame into coincidence with the PPMXL frame on magnitude. Fig. 5 shows the m -dependent rotation angles of the UCAC4 on PPMXL Galactic reference frames around the poles with longitudes and latitudes for various magnitudes. In the same figure, we can see a map of the vector field, which corresponds to $J = 13$ systematic differences of Galactic coordinates. In the same way, Fig. 6 shows the m -dependent angular velocities of the UCAC4 on PPMXL Galactic reference frames around the poles with longitudes and latitudes for various magnitudes. We can see that the angular velocity reaches the biggest value at $J = 13$ –14. In the same

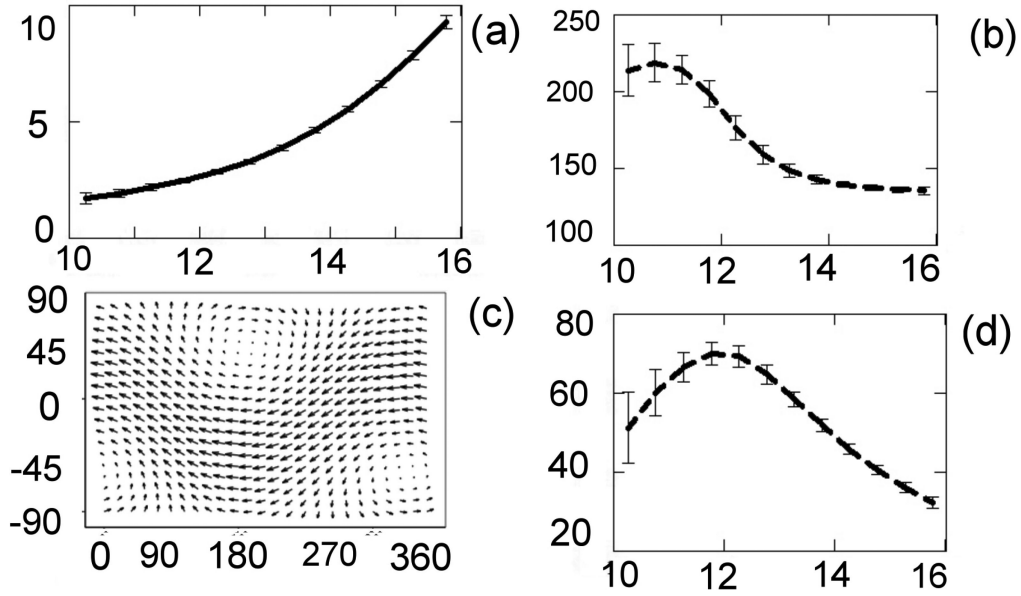


Figure 5. (a) Rotation angles (mas) of UCAC4 on the PPMXL Galactic reference frames around the pole whose longitudes and latitudes in degrees are shown in panels (b) and (d). The J magnitudes of the samples are along the horizontal axes. (c) The vector field of systematic differences $\Delta l/\cos b$ and Δb corresponds to the position of the pole at $J = 13$ mag. The longitudes (deg) and latitudes (deg) are along the horizontal and vertical axes, respectively.

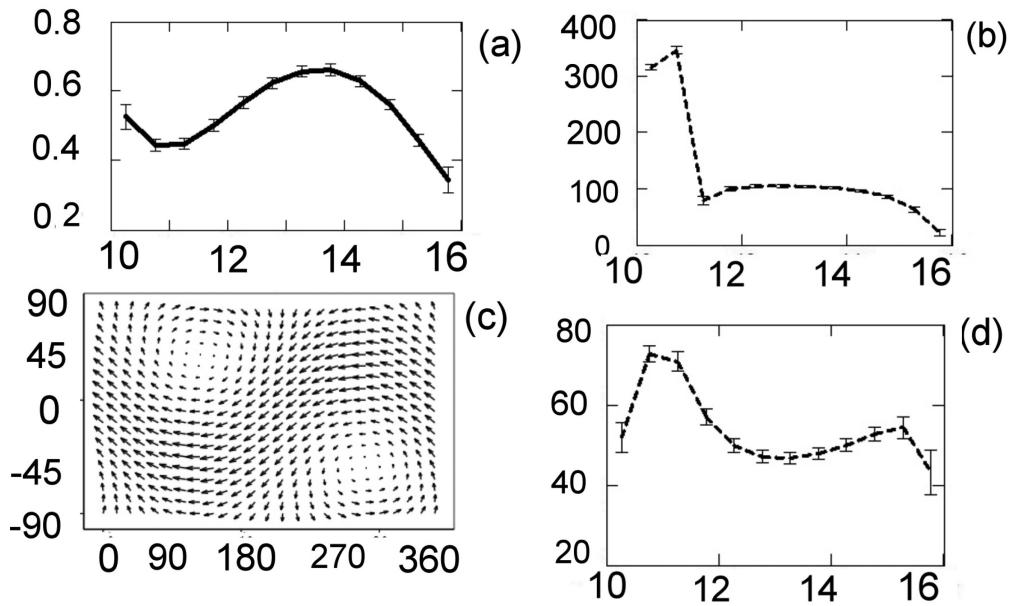


Figure 6. (a) Velocity of rotation (mas yr^{-1}) of UCAC4 on the PPMXL Galactic reference frames around the pole whose longitudes and latitudes are shown in panels (b) and (d). The J magnitudes of the samples are along the horizontal axes. (c) The vector field of systematic differences $\Delta \mu_l \cos b$ and $\Delta \mu_b$ corresponds to the position of the pole at $J = 13$ mag. The longitudes (deg) and latitudes (deg) are along the horizontal and vertical axes, respectively.

figure, we can see a map of the vector field, which corresponds to $J = 13$ systematic differences of Galactic proper motions as well as the coordinates of the pole. It is worth mentioning that the axis of mutual rotation practically does not change its orientation in the range $12 < J < 14$ mag.

It should be said that the systematic stellar position and proper motion differences PPMXL–UCAC4 show a pronounced dependence on the magnitude of stars. This manifests itself in the fact that almost all coefficients t_{nkp} and s_{nkp} are functions of the magnitude (Tables 3 and 4). From Figs 5 and 6 we can see that the mutual

rotation angles of the PPMXL and UCAC4 reference frames change for different magnitude groups and can reach 10 mas, while the rate of mutual rotation can reach 0.7 mas yr^{-1} . The disagreement of both Galactic frames is explained by the differences of the equatorial frames of PPMXL and UCAC4 as no attempts were made to construct each Galactic frame in the systems of each catalogue under consideration.

The standard Galactic coordinate system currently in use was introduced by the International Astronomical Union (IAU) in 1958 (Blaauw et al. 1960). The attempts to construct a Galactic

coordinate system based on modern near-infrared and radio catalogues (Liu, Zhu & Hu 2011) give the corrections to the position of the Galactic plane at the level of several arcmin. From this point of view, the milliarcsec discrepancies between the PPMXL and UCAC4 Galactic coordinate systems found in this paper are quite negligible with respect to the accuracy of the standard system itself. Obviously, these small PPMXL and UCAC4 differences will be preserved in any new standard system of Galactic coordinates.

6.1 Kinematic analysis of the systematic differences between proper motions

In this section, we study the influence of systematic differences of proper motions on the determination of the kinematic parameters of the stellar velocity field.

The equations of the Ogorodnikov–Milne model (Ogorodnikov 1965) are commonly used to investigate the kinematics of stars. In this model, the stellar velocity field is represented by the linear expression

$$\mathbf{V} = \mathbf{V}_0 + \boldsymbol{\Omega} \times \mathbf{r} + \mathbf{M}^+ \mathbf{r}, \quad (41)$$

where \mathbf{V} is the stellar velocity, \mathbf{V}_0 is the effect of the translational Solar motion, $\boldsymbol{\Omega}$ is the angular velocity of rigid-body rotation of the stellar system and \mathbf{M}^+ is the symmetric velocity field deformation tensor.

The Ogorodnikov–Milne model contains 12 parameters, as follows.

U , V and W are the components of the velocity vector of translational Solar motion \mathbf{V}_0 relative to the stars.

Ω_x , Ω_y and Ω_z are the components of the vector of rigid-body rotation $\boldsymbol{\Omega}$.

M_{11}^+ , M_{22}^+ and M_{33}^+ are the parameters of the tensor \mathbf{M}^+ that describe the velocity field contraction-expansion along the principal Galactic axes.

M_{12}^+ , M_{13}^+ and M_{23}^+ are the parameters of the tensor \mathbf{M}^+ that describe the velocity field deformation in the principal plane and in the two planes perpendicular to it.

Projecting equation (41) onto the unit vectors of the Galactic coordinate system (where r denotes the distance to the star and $\mathcal{K} = 4.738$ is used to convert dimensions mas yr^{-1} into $\text{km s}^{-1} \text{kpc}^{-1}$), we obtain

$$\begin{aligned} \mathcal{K}\mu_l \cos b &= U/r \sin l - V/r \cos l - \Omega_x \sin b \cos l \\ &\quad - \Omega_y \sin b \sin l + \Omega_z \cos b - M_{13}^+ \sin b \sin l \\ &\quad + M_{23}^+ \sin b \cos l + M_{12}^+ \cos b \cos l \\ &\quad - \frac{1}{2} M_{11}^+ \cos b \sin 2l + \frac{1}{2} M_{22}^+ \cos b \sin 2l \end{aligned} \quad (42)$$

and

$$\begin{aligned} \mathcal{K}\mu_b &= U/r \cos l \sin b + V/r \sin l \sin b - W/r \cos b \\ &\quad + \Omega_x \sin l - \Omega_y \cos l - \frac{1}{2} M_{12}^+ \sin 2b \sin 2l \\ &\quad + M_{13}^+ \cos 2b \cos l + M_{23}^+ \cos 2b \sin l \\ &\quad - \frac{1}{2} M_{11}^+ \sin 2b \cos^2 l - \frac{1}{2} M_{22}^+ \sin 2b \sin^2 l \\ &\quad + \frac{1}{2} M_{33}^+ \sin 2b. \end{aligned} \quad (43)$$

Table 5. The VSH expansion coefficients of the proper motion differences $\mathcal{K}\Delta\mu_\alpha \cos \delta e_l + \mathcal{K}\Delta\mu_\delta e_b$ and their connections with the differences of the Ogorodnikov–Milne kinematic parameters.

Coefficient	Kinematical meaning
t_{101}	$2.89 \Delta\Omega_z$
t_{110}	$2.89 \Delta\Omega_y$
t_{111}	$2.89 \Delta\Omega_x$
s_{101}	$-2.89 \Delta W/\langle r \rangle$
s_{110}	$-2.89 \Delta V/\langle r \rangle$
s_{111}	$-2.89 \Delta U/\langle r \rangle$
s_{201}	$-0.65 (\Delta M_{11}^+ + \Delta M_{22}^+ - 2\Delta M_{33}^+)$
s_{210}	$2.24 \Delta M_{23}^+$
s_{211}	$2.24 \Delta M_{13}^+$
s_{220}	$2.24 \Delta M_{12}^+$
s_{221}	$1.12 \Delta M_{11}^+$

It is worth noting that the right-hand sides of these equations can be expressed in terms of VSH as

$$\begin{aligned} \mathcal{K}\mu_l \cos b e_l + \mathcal{K}\mu_b e_b &= \\ &= -U/r \frac{\mathbf{S}_{111}(l, b)}{\rho_{11}} - V/r \frac{\mathbf{S}_{110}(l, b)}{\rho_{11}} - W/r \frac{\mathbf{S}_{101}(l, b)}{\rho_{10}} \\ &\quad + \Omega_x \frac{\mathbf{T}_{111}(l, b)}{\rho_{11}} + \Omega_y \frac{\mathbf{T}_{110}(l, b)}{\rho_{11}} + \Omega_z \frac{\mathbf{T}_{101}(l, b)}{\rho_{10}} \\ &\quad + \frac{M_{13}^+}{3} \frac{\mathbf{S}_{211}(l, b)}{\rho_{21}} + \frac{M_{23}^+}{3} \frac{\mathbf{S}_{210}(l, b)}{\rho_{21}} + \frac{M_{12}^+}{6} \frac{\mathbf{S}_{220}(l, b)}{\rho_{22}} \\ &\quad + \frac{M_{11}^+}{12} \frac{\mathbf{S}_{221}(l, b)}{\rho_{22}} + \frac{X}{3} \frac{\mathbf{S}_{201}(l, b)}{\rho_{20}}, \end{aligned} \quad (44)$$

where

$$\rho_{nk} = \sqrt{\frac{2n+1}{4\pi n(n+1)}} \begin{cases} \sqrt{\frac{2(n-k)!}{(n+k)!}}, & k > 0 \\ 1, & k = 0 \end{cases} \quad (45)$$

and

$$M_{11}^* = M_{11}^+ - M_{22}^+, \quad (46)$$

$$X = M_{33}^+ - \frac{1}{2} (M_{11}^+ + M_{22}^+). \quad (47)$$

Now we see that the VSH coefficients of the expansion of equation (44) are simply proportional to the parameters of the Ogorodnikov–Milne model. In our previous paper (Vityazev & Tsvetkov 2009), we found the relations connecting the expansion VSH coefficients with the parameters of the Ogorodnikov–Milne model. It is obvious that because the Ogorodnikov–Milne equations are linear, the systematic differences of the proper motions can be represented by the same equations with parameters $\Delta U/r$, $\Delta V/r$, \dots , ΔM_{33}^+ instead of U/r , V/r , \dots , M_{33}^+ . In this way, the connections of the systematic differences of expansion coefficients with the differences of the kinematic parameters are shown in Table 5. It should be kept in mind that the components of the solar motion enter into equations (42) and (43) with the factor $1/r$. For this reason, we can determine the parameters of the solar motion only to within the factor $1/\langle r \rangle$, where $\langle r \rangle$ is the average distance to the stars.

From Table 5 we can conclude the following.

(i) The first-order spheroidal coefficients s_{101} , s_{110} and s_{111} are generated by the differences of the solar motion components referring to the average distance to the stars $\Delta W/\langle r \rangle$, $\Delta U/\langle r \rangle$ and $\Delta V/\langle r \rangle$.

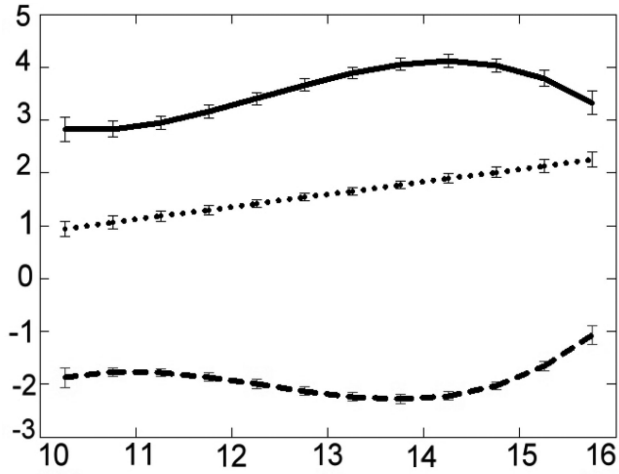


Figure 7. The Oort constant differences ΔA (dotted line) and ΔB (dashed line) and differences of the Galactic angular velocity rotation (solid line) against J magnitude on the horizontal axis. Units are $\text{km s}^{-1} \text{kpc}^{-1}$.

(ii) The first-order toroidal coefficients t_{101} , t_{110} and t_{111} are produced by the differences of the rigid body rotation vector components $\Delta\Omega_z$, $\Delta\Omega_y$ and $\Delta\Omega_x$.

(iii) The second-order spheroidal coefficient s_{201} is a linear combination of the terms describing the differences of velocity field contraction–expansion along the principal Galactic axes.

(iv) The first-order spheroidal coefficients s_{210} , s_{211} and s_{220} are the contributions to the systematic differences between the proper motions of the differences ΔM_{23}^+ , ΔM_{13}^+ and ΔM_{12}^+ , which describe the differential velocity field deformations in the principal plane and in the two planes perpendicular to it.

(v) The second-order spheroidal coefficient s_{221} is generated by the difference of the parameters $\Delta M_{11}^+ - \Delta M_{22}^+$, each of which describes the deformations of the velocity field along the x - and y -axes.

It is clear that the differences of the Oort constants A and B derived from our catalogues can be calculated via the toroidal and spheroidal coefficients in the representation of the proper motion systematic differences of these catalogues according to simple relations (Vityazev & Tsvetkov 2009, 2014):

$$\Delta A = \frac{\mathcal{K}}{2.24} s_{220} \quad \text{and} \quad \Delta B = \frac{\mathcal{K}}{2.89} t_{101}. \quad (48)$$

Now, for the difference of the Galactic angular velocity rotation, derived from the catalogues, we have

$$\Delta\Omega_G = \Delta A - \Delta B. \quad (49)$$

The dependence of these values on magnitude is shown in Fig. 7. It is easy to see that the effect of the magnitude equation is small, that is why the variation of the Oort constants and the angular velocity of the Galaxy’s rotation in the vicinity of the Sun can be evaluated by the mean values $\langle\Delta A\rangle = 1.60 \pm 0.41$, $\langle\Delta B\rangle = -1.91 \pm 0.32$ and $\langle\Delta\Omega_G\rangle = 3.51 \pm 0.52 \text{ km s}^{-1} \text{kpc}^{-1}$. These offsets significantly exceed the accuracy of the determination of the Oort constants A and B themselves, which are at the level of $0.1\text{--}0.2 \text{ km s}^{-1} \text{kpc}^{-1}$ (Vityazev & Tsvetkov 2014). Thus, the systematic differences of the proper motions in the PPMXL and UCAC4 catalogues can be a source of various values of the Oort constants derived from these catalogues.

7 CONCLUSIONS

In this paper, we obtain the systematic differences between the Galactic positions and proper motions of stars of the extensive modern astrometric catalogues, PPMXL and UCAC4. The systematic differences are expressed in terms of the VSH. To extract the signal from the noise, the chi-square criterion was proposed with orientation on the HEALPIX method of the data pre-pixelization. The criterion is able to test the significance of all harmonics, which can be calculated with pixelization chosen. We used an analytical method to take into consideration the magnitude equation proposed in our previous paper (Vityazev & Tsvetkov 2015). This gave a new model of systematic differences with basis functions constructed by the combination of VSH and Legendre polynomials. To our knowledge, this is the first ever attempt to study the systematic differences of positions and proper motions of two catalogues in the Galactic coordinate system, aiming at the study of stellar kinematics. The physical meaning of the VSH decomposition coefficients of the systematic differences is clarified. This is a general result valid for any pair of catalogues.

The calculated coefficients of the representation of the differences between positions and proper motions in terms of the introduced functions in the Galactic coordinate system can be used to reduce the positions and proper motions of one catalogue to the system of another catalogue. The systematic differences were used for analysis of the PPMXL and UCAC4 Galactic reference frames. The mutual orientation of the frames under consideration and the rate of their mutual rotation depend on magnitude and can reach the level of 10 mas for orientation and 0.7 mas yr^{-1} for their mutual spin. Beside this, the kinematic analysis of the low-order harmonics (up to $n = 2$) of the representations of the proper motions on VSH was made. This shows the influence of the systematic differences on determination of the parameters of the linear Ogorodnikov–Milne model.

The theory and numerical results were obtained using real vector harmonics. A set of equations is derived that allows us to convert these results into an expression that would have occurred if the complex spherical harmonics were used.

ACKNOWLEDGEMENTS

This work was carried out with the support of the St Petersburg University Grant 6.37.343.2015. The authors are grateful to the Scientific Editor and to reviewers for their remarks, which helped to improve the paper.

REFERENCES

- Bien R., Fricke W., Lederle T., Schwan H., 1978, Veroff. Heidelberg Astron. Rech.-Inst., 29, 1
- Blaauw A., Gum C. S., Pawsey J. L., Westerhout G., 1960, MNRAS, 121, 123
- Brosche P., 1966, Veroff. Heidelberg Astron. Rech.-Inst., 17, 1
- Farnocchia D., Chesley S. R., Chamberlin A. B., Tholen D. J., 2015, Icarus, 245, 94
- Fedorov P. N., Myznikov A. A., Akhmetov V. S., 2009, MNRAS, 393, 133
- Froeschle M., Kovalevsky J., 1982, A&A, 116, 89
- Gorski K. M., Hivon E., Banday A. J., Wandelt B. D., Hansen F. K., Reinecke M., Bartelmann M., 2005, ApJ, 622, 759
- Liu J.-C., Zhu Z., Hu B., 2011, A&A, 536, A102
- Mignard F., 2000, A&A, 354, 522
- Mignard F., Klioner S., 2012, A&A, 547, A59
- Mignard F., Morando B., 1990, in Journées 90: Systèmes de Référence Spatio-Temporels. Paris, p. 151
- Ogorodnikov K., 1965, Dynamics of Stellar Systems. Pergamon, Oxford

- Roeser S., Demleitner M., Schilbach E., 2010, *AJ*, 139, 2440
 Skrutskie M. F. et al., 2006, *AJ*, 131, 1163
 Vityazev V., 1989, *Vestnik Leningr. Univ.*, Ser. 1, Iss. 2, 8, 73
 Vityazev V., 1993, *A&A Trans.*, 4, 195
 Vityazev V., Tsvetkov A., 2009, *Astron. Lett.*, 35, 100
 Vityazev V., Tsvetkov A., 2013, *AN*, 334, 760
 Vityazev V. V., Tsvetkov A. S., 2014, *MNRAS*, 442, 1249
 Vityazev V., Tsvetkov A., 2015, *Astron. Lett.*, 41, 317
 Zacharias N., Finch C. T., Girard T. M., Henden A., Bartlett J. L., Monet
 D. G., Zacharias M. I., 2013, *AJ*, 145, 44

APPENDIX A: REAL AND COMPLEX SPHERICAL HARMONICS

A1 Scalar spherical harmonics

The VSH formalism in this paper is based on the real spherical harmonics K_{nkp} defined as

$$K_{nkp}(\alpha, \delta) = R_{nk} \begin{cases} P_{n,0}(\delta), & k = 0, & p = 1 \\ P_{nk}(\delta) \sin k\alpha, & k \neq 0, & p = 0 \\ P_{nk}(\delta) \cos k\alpha, & k \neq 0, & p = 1 \end{cases} \quad (\text{A1})$$

and

$$R_{nk} = \sqrt{\frac{2n+1}{4\pi}} \begin{cases} \sqrt{\frac{2(n-k)!}{(n+k)!}}, & k > 0 \\ 1, & k = 0 \end{cases}. \quad (\text{A2})$$

Here, α and δ are the RA (longitude) and Dec. (latitude) of a point on the sphere, respectively ($0 \leq \alpha \leq 2\pi$; $-\pi/2 \leq \delta \leq \pi/2$), and $P_{nk}(\delta)$ are Legendre polynomials (at $k = 0$) and associated Legendre functions (at $k > 0$), which can be calculated using the following recurrence relations:

$$P_{nk}(\delta) = \sin \delta \frac{2n-1}{n-k} P_{n-1,k}(\delta) - \frac{n+k-1}{n-k} P_{n-2,k}(\delta),$$

$$k = 0, 1, \dots; n = k+2, k+3, \dots$$

Table A1. Explicit formulae for the real spherical harmonics $K_{nkp}(\alpha, \delta)$ up to $n = 3$. The harmonics are numbered with $j = n^2 + 2k + p - 1$.

	$n = 0$	$n = 1$	$n = 2$	$n = 3$
$k = 3$ $p = 1$				$\sqrt{\frac{35}{32\pi}} \cos^3 \delta \cos 3\alpha$ $j = 15$
$k = 3$ $p = 0$				$\sqrt{\frac{35}{32\pi}} \cos^3 \delta \sin 3\alpha$ $j = 14$
$k = 2$ $p = 1$			$\sqrt{\frac{15}{16\pi}} \cos^2 \delta \cos 2\alpha$ $j = 8$	$\sqrt{\frac{105}{16\pi}} \sin \delta \cos^2 \delta \cos 2\alpha$ $j = 13$
$k = 2$ $p = 0$			$\sqrt{\frac{15}{16\pi}} \cos^2 \delta \sin 2\alpha$ $j = 7$	$\sqrt{\frac{105}{16\pi}} \sin \delta \cos^2 \delta \sin 2\alpha$ $j = 12$
$k = 1$ $p = 1$		$\sqrt{\frac{3}{4\pi}} \cos \delta \cos \alpha$ $j = 3$	$\sqrt{\frac{15}{16\pi}} \sin 2\delta \cos \alpha$ $j = 6$	$\sqrt{\frac{21}{32\pi}} \cos \delta (5 \sin^2 \delta - 1) \cos \alpha$ $j = 11$
$k = 1$ $p = 0$		$\sqrt{\frac{3}{4\pi}} \cos \delta \sin \alpha$ $j = 2$	$\sqrt{\frac{15}{16\pi}} \sin 2\delta \sin \alpha$ $j = 5$	$\sqrt{\frac{21}{32\pi}} \cos \delta (5 \sin^2 \delta - 1) \sin \alpha$ $j = 10$
$k = 0$ $p = 1$	$\sqrt{\frac{1}{4\pi}}$ $j = 0$	$\sqrt{\frac{3}{4\pi}} \sin \delta$ $j = 1$	$\sqrt{\frac{5}{16\pi}} (3 \sin^2 \delta - 1)$ $j = 4$	$\sqrt{\frac{7}{16\pi}} (5 \sin^3 \delta - 3 \sin \delta)$ $j = 9$

$$P_{kk}(\delta) = \frac{(2k)!}{2^k k!} \cos^k \delta,$$

$$P_{k+1,k}(\delta) = \frac{(2k+2)!}{2^{k+1}(k+1)!} \cos^k \delta \sin \delta. \quad (\text{A3})$$

Very often, one index j instead of three indices nkp is used for the convenience of the numbering of the spherical harmonics, with

$$j = n^2 + 2k + p - 1. \quad (\text{A4})$$

The introduced functions satisfy the relation

$$\int_{\Omega} (K_i \cdot K_j) d\omega = \begin{cases} 0, & i \neq j \\ 1, & i = j \end{cases}. \quad (\text{A5})$$

In other words, the set of functions K_{nkp} forms an orthonormal system of functions on the sphere. Explicit formulae for the spherical harmonics $K_{nkp}(\alpha, \delta)$ up to $n = 3$ are shown in Table A1. The real spherical harmonics were introduced into the problem of systematic differences by Brosche (1966).

Meanwhile, in many applications, the complex form of the spherical harmonics is used (Mignard & Klioner 2012):

$$Y_{nk}(\alpha, \delta) = \tilde{R}_{nk} \begin{cases} P_{n,0}(\delta), & k = 0 \\ (-1)^k P_{nk}(\delta) \exp(ik\alpha), & k > 0; \\ P_{n|k|}(\delta) \exp(-i|k|\alpha), & k < 0 \end{cases} \quad (\text{A6})$$

$$\tilde{R}_{nk} = \sqrt{\frac{2n+1}{4\pi}} \begin{cases} \sqrt{\frac{(n-|k|)!}{(n+|k|)!}}, & k \neq 0 \\ 1, & k = 0 \end{cases}. \quad (\text{A7})$$

Explicit formulae for these harmonics ($n \leq 3$) are shown in Table A2.

Table A2. Explicit formulae for the complex spherical harmonics $Y_{nk}(\alpha, \delta)$ up to $n = 3$.

	$n = 0$	$n = 1$	$n = 2$	$n = 3$
$k = 3$				$-\sqrt{\frac{35}{64\pi}} \cos^3 \delta e^{i3\alpha}$
$k = 2$			$\sqrt{\frac{15}{32\pi}} \cos^2 \delta e^{i2\alpha}$	$\sqrt{\frac{105}{32\pi}} \sin \delta \cos^2 \delta e^{i2\alpha}$
$k = 1$		$-\sqrt{\frac{3}{8\pi}} \cos \delta e^{i\alpha}$	$-\sqrt{\frac{15}{32\pi}} \sin 2\delta e^{i\alpha}$	$-\sqrt{\frac{21}{64\pi}} \cos \delta (5 \sin^2 \delta - 1) e^{i\alpha}$
$k = 0$	$\sqrt{\frac{1}{4\pi}}$	$\sqrt{\frac{3}{4\pi}} \sin \delta$	$\sqrt{\frac{5}{16\pi}} (3 \sin^2 \delta - 1)$	$\sqrt{\frac{7}{16\pi}} (5 \sin^3 \delta - 3 \sin \delta)$
$k = -1$		$\sqrt{\frac{3}{8\pi}} \cos \delta e^{-i\alpha}$	$\sqrt{\frac{15}{32\pi}} \sin 2\delta e^{-i\alpha}$	$\sqrt{\frac{21}{64\pi}} \cos \delta (5 \sin^2 \delta - 1) e^{-i\alpha}$
$k = -2$			$\sqrt{\frac{15}{32\pi}} \cos^2 \delta e^{-i2\alpha}$	$\sqrt{\frac{105}{32\pi}} \sin \delta \cos^2 \delta e^{-i2\alpha}$
$k = -3$				$\sqrt{\frac{35}{64\pi}} \cos^3 \delta e^{-i3\alpha}$

Comparison of equation (A6) with equation (A1) yields ‘complex from real’ transforms to express complex spherical harmonics $Y_{nk}(\alpha, \delta)$ via real harmonics $K_{nkp}(\alpha, \delta)$:

$$Y_{nk} = \begin{cases} K_{n01}, & k = 0 \\ \frac{(-1)^k}{\sqrt{2}} (K_{nk1} + iK_{nk0}), & k > 0 \\ \frac{1}{\sqrt{2}} (K_{n|k|1} - iK_{n|k|0}), & k < 0 \end{cases} \quad (\text{A8})$$

The inverse relations ‘real from complex’, which allow us to obtain real functions via complex ones, are

$$K_{nkp} = \begin{cases} Y_{n,k}, & k = 0, p = 1 \\ (-1)^k \sqrt{2} \operatorname{Re} Y_{n,k} & k > 0, p = 1 \\ (-1)^k \sqrt{2} \operatorname{Im} Y_{n,k} & k > 0, p = 0 \end{cases} \quad (\text{A9})$$

A2 Vector spherical harmonics

Consider a system of mutually orthogonal unit vectors $\mathbf{e}_\alpha, \mathbf{e}_\delta$, respectively, in the directions of change in RA (longitude) and Dec. (latitude) in a plane tangential to the sphere. The real VSH are introduced with the toroidal, \mathbf{T}_{nkp} , and spheroidal, \mathbf{S}_{nkp} functions via the relations

$$\mathbf{T}_j = \frac{1}{\sqrt{n(n+1)}} \left[\frac{\partial K_j(\alpha, \delta)}{\partial \delta} \mathbf{e}_\alpha - \frac{1}{\cos \delta} \frac{\partial K_j(\alpha, \delta)}{\partial \alpha} \mathbf{e}_\delta \right] \quad (\text{A10})$$

and

$$\mathbf{S}_j = \frac{1}{\sqrt{n(n+1)}} \left[\frac{1}{\cos \delta} \frac{\partial K_j(\alpha, \delta)}{\partial \alpha} \mathbf{e}_\alpha + \frac{\partial K_j(\alpha, \delta)}{\partial \delta} \mathbf{e}_\delta \right]. \quad (\text{A11})$$

We denote the components of the unit vector \mathbf{e}_α as T_{nkp}^α and S_{nkp}^α , and the components of the unit vector \mathbf{e}_δ as T_{nkp}^δ and S_{nkp}^δ :

$$\mathbf{T}_{nkp} = T_{nkp}^\alpha \mathbf{e}_\alpha + T_{nkp}^\delta \mathbf{e}_\delta; \quad (\text{A12})$$

$$\mathbf{S}_{nkp} = S_{nkp}^\alpha \mathbf{e}_\alpha + S_{nkp}^\delta \mathbf{e}_\delta. \quad (\text{A13})$$

Given that $P_{n,k+1}(b) = 0$ at $n < k + 1$, these components are defined as

$$T_j^\alpha = S_j^\delta = \rho_{nk} \begin{cases} P_{n,1}(\delta), & k = 0, p = 1 \\ (-k \tan \delta P_{nk}(\delta) + P_{n,k+1}(\delta)) \\ \times \sin k\alpha, & k \neq 0, p = 0 \\ (-k \tan \delta P_{nk}(\delta) + P_{n,k+1}(\delta)) \\ \times \cos k\alpha, & k \neq 0, p = 1 \end{cases} \quad (\text{A14})$$

and

$$T_j^\delta = -S_j^\alpha = \rho_{nk} \begin{cases} 0, & k \neq 0, p = 1 \\ -\frac{k}{\cos \delta} P_{nk}(\delta) \cos k\alpha, & k \neq 0, p = 0 \\ +\frac{k}{\cos \delta} P_{nk}(\delta) \sin k\alpha, & k \neq 0, p = 1 \end{cases}, \quad (\text{A15})$$

where

$$\rho_{nk} = \frac{R_{nk}}{\sqrt{n(n+1)}}. \quad (\text{A16})$$

The introduced functions satisfy the relations:

$$\int_{\Omega} (\mathbf{T}_i \cdot \mathbf{T}_j) d\omega = \int_{\Omega} (\mathbf{S}_i \cdot \mathbf{S}_j) d\omega = \begin{cases} 0, & i \neq j \\ 1, & i = j \end{cases}; \quad (\text{A17})$$

$$\int_{\Omega} (\mathbf{S}_i \cdot \mathbf{T}_j) d\omega = 0, \quad \forall i, j. \quad (\text{A18})$$

In other words, the set of functions \mathbf{T}_{nkp} and \mathbf{S}_{nkp} forms an orthonormal system of functions on the sphere. The explicit expressions for real VSH $T_{nkp}(\alpha, \delta)$ and $S_{nkp}(\alpha, \delta)$ up to $n = 3$ are shown in Tables A3 and A4.

With the complex form of the VSH we introduce magnetic \mathbf{M}_{nk} and electric \mathbf{E}_{nk} VSH:

$$\mathbf{M}_{nk}(\alpha, \delta) = r_n \left[\frac{\partial Y_{nk}(\alpha, \delta)}{\partial \delta} \mathbf{e}_\alpha - \frac{1}{\cos \delta} \frac{\partial Y_{nk}(\alpha, \delta)}{\partial \alpha} \mathbf{e}_\delta \right], \quad (\text{A19})$$

$$\mathbf{E}_{nk}(\alpha, \delta) = r_n \left[\frac{1}{\cos \delta} \frac{\partial Y_{nk}(\alpha, \delta)}{\partial \alpha} \mathbf{e}_\alpha + \frac{\partial Y_{nk}(\alpha, \delta)}{\partial \delta} \mathbf{e}_\delta \right], \quad (\text{A20})$$

Table A3. Real VSH $T_{nkp}(\alpha, \delta)$ up to $n = 3$.

T_{nkp}	Coefficient	T_{nkp}^α	T_{nkp}^δ
$T_{1,0,1}$	$\sqrt{\frac{3}{8\pi}}$	$\cos \delta$	0
$T_{2,0,1}$	$\sqrt{\frac{15}{32\pi}}$	$\sin 2\delta$	0
$T_{3,0,1}$	$\sqrt{\frac{21}{64\pi}}$	$\cos \delta(5\sin^2 \delta - 1)$	0
$T_{1,1,0}$	$-\sqrt{\frac{3}{8\pi}}$	$\sin \delta \sin \alpha$	$\cos \alpha$
$T_{1,1,1}$	$-\sqrt{\frac{3}{8\pi}}$	$\sin \delta \cos \alpha$	$-\sin \alpha$
$T_{2,1,0}$	$\sqrt{\frac{5}{8\pi}}$	$\cos 2\delta \sin \alpha$	$-\sin \delta \cos \alpha$
$T_{2,1,1}$	$\sqrt{\frac{5}{8\pi}}$	$\cos 2\delta \cos \alpha$	$\sin \delta \sin \alpha$
$T_{2,2,0}$	$-\sqrt{\frac{5}{32\pi}}$	$\sin 2\delta \sin 2\alpha$	$2\cos \delta \cos 2\alpha$
$T_{2,2,1}$	$-\sqrt{\frac{5}{32\pi}}$	$\sin 2\delta \cos 2\alpha$	$-2\cos \delta \sin 2\alpha$
$T_{3,1,0}$	$-\sqrt{\frac{7}{128\pi}}$	$(15\sin^2 \delta - 11)\sin \delta \sin \alpha$	$(5\sin^2 \delta - 1)\cos \alpha$
$T_{3,1,1}$	$-\sqrt{\frac{7}{128\pi}}$	$(15\sin^2 \delta - 11)\sin \delta \cos \alpha$	$-(5\sin^2 \delta - 1)\sin \alpha$
$T_{3,2,0}$	$\sqrt{\frac{35}{64\pi}}$	$(1 - 3\sin^2 \delta)\cos \delta \sin 2\alpha$	$-\sin 2\delta \cos 2\alpha$
$T_{3,2,1}$	$\sqrt{\frac{35}{64\pi}}$	$(1 - 3\sin^2 \delta)\cos \delta \cos 2\alpha$	$\sin 2\delta \sin 2\alpha$
$T_{3,3,0}$	$-\sqrt{\frac{105}{128\pi}}$	$\sin \delta \cos^2 \delta \sin 3\alpha$	$\cos^2 \delta \cos 3\alpha$
$T_{3,3,1}$	$-\sqrt{\frac{105}{128\pi}}$	$\sin \delta \cos^2 \delta \cos 3\alpha$	$-\cos^2 \delta \sin 3\alpha$

where $Y_{nk}(\alpha, \delta)$ is given by equation (A6) and

$$r_n = \frac{1}{\sqrt{n(n+1)}}. \quad (\text{A21})$$

It is obvious that the magnetic and electric functions are the analogues of the toroidal and spheroidal functions introduced earlier. Explicit formulae for these complex spherical harmonics up to $n = 3$ and $k \geq 0$ are shown in Tables A5 and A6. For negative values of index k , the following relations are valid:

$$\mathbf{M}_{n,-k}(\alpha, \delta) = (-1)^k \mathbf{M}_{n,k}^*(\alpha, \delta), \quad (\text{A22})$$

$$\mathbf{E}_{n,-k}(\alpha, \delta) = (-1)^k \mathbf{E}_{n,k}^*(\alpha, \delta), \quad (\text{A23})$$

where the superscript ‘*’ denotes complex conjugation.

By comparing equations (A10) and (A11) with equations (A19) and (A20), we obtain the relations of ‘magnetic and electric via toroidal and spheroidal’ functions

$$\mathbf{M}_{nk} = \begin{cases} T_{n01}^\alpha, & k = 0 \\ \frac{(-1)^k}{\sqrt{2}} (T_{nk1}^\alpha + iT_{nk0}^\alpha) \mathbf{e}_\alpha \\ + \frac{(-1)^k}{\sqrt{2}} (T_{nk1}^\delta + iT_{nk0}^\delta) \mathbf{e}_\delta, & k > 0 \\ \frac{1}{\sqrt{2}} (T_{n|k|1}^\alpha - iT_{n|k|0}^\alpha) \mathbf{e}_\alpha \\ + \frac{1}{\sqrt{2}} (T_{n|k|1}^\delta - iT_{n|k|0}^\delta) \mathbf{e}_\delta, & k < 0 \end{cases} \quad (\text{A24})$$

and

$$\mathbf{E}_{nk} = \begin{cases} S_{n01}^\alpha, & k = 0 \\ \frac{(-1)^k}{\sqrt{2}} (S_{nk1}^\alpha + iS_{nk0}^\alpha) \mathbf{e}_\alpha \\ + \frac{(-1)^k}{\sqrt{2}} (S_{nk1}^\delta + iS_{nk0}^\delta) \mathbf{e}_\delta, & k > 0. \\ \frac{1}{\sqrt{2}} (S_{n|k|1}^\alpha - iS_{n|k|0}^\alpha) \mathbf{e}_\alpha \\ + \frac{1}{\sqrt{2}} (S_{n|k|1}^\delta - iS_{n|k|0}^\delta) \mathbf{e}_\delta, & k < 0 \end{cases} \quad (\text{A25})$$

In what follows, we use the representations

$$\mathbf{M}_{nk} = M_{nk}^\alpha \mathbf{e}_\alpha + M_{nk}^\delta \mathbf{e}_\delta \quad (\text{A26})$$

and

$$\mathbf{S}_{nk} = S_{nk}^\alpha \mathbf{e}_\alpha + S_{nk}^\delta \mathbf{e}_\delta. \quad (\text{A27})$$

With these notations, the inverse relations of ‘toroidal and spheroidal from magnetic and electric’ harmonics are

$$T_{nkp}^\alpha = \begin{cases} M_{n,k}^\alpha, & k = 0, p = 1 \\ (-1)^k \sqrt{2} \operatorname{Re} M_{n,k}^\alpha & k > 0, p = 1; \\ (-1)^k \sqrt{2} \operatorname{Im} M_{n,k}^\alpha & k > 0, p = 0 \end{cases} \quad (\text{A28})$$

$$T_{nkp}^\delta = \begin{cases} M_{n,k}^\delta, & k = 0, p = 1 \\ (-1)^k \sqrt{2} \operatorname{Re} M_{n,k}^\delta & k > 0, p = 1; \\ (-1)^k \sqrt{2} \operatorname{Im} M_{n,k}^\delta & k > 0, p = 0 \end{cases} \quad (\text{A29})$$

Table A4. Real VSH $S_{nkp}(\alpha, \delta)$ up to $n = 3$.

T_{nkp}	Coeff.	S_{nkp}^α	S_{nkp}^δ
$S_{1,0,1}$	$\sqrt{\frac{3}{8\pi}}$	0	$\cos \delta$
$S_{2,0,1}$	$\sqrt{\frac{15}{32\pi}}$	0	$\sin 2\delta$
$S_{3,0,1}$	$\sqrt{\frac{21}{64\pi}}$	0	$\cos \delta(5\sin^2 \delta - 1)$
$S_{1,1,0}$	$-\sqrt{\frac{3}{8\pi}}$	$-\cos \alpha$	$\sin \delta \sin \alpha$
$S_{1,1,1}$	$-\sqrt{\frac{3}{8\pi}}$	$\sin \alpha$	$\sin \delta \cos \alpha$
$S_{2,1,0}$	$\sqrt{\frac{5}{8\pi}}$	$\sin \delta \cos \alpha$	$\cos 2\delta \sin \alpha$
$S_{2,1,1}$	$\sqrt{\frac{5}{8\pi}}$	$-\sin \delta \sin \alpha$	$\cos 2\delta \cos \alpha$
$S_{2,2,0}$	$-\sqrt{\frac{5}{32\pi}}$	$-2\cos \delta \cos 2\alpha$	$\sin 2\delta \sin 2\alpha$
$S_{2,2,1}$	$-\sqrt{\frac{5}{32\pi}}$	$2\cos \delta \sin 2\alpha$	$\sin 2\delta \cos 2\alpha$
$S_{3,1,0}$	$-\sqrt{\frac{7}{128\pi}}$	$-(5\sin^2 \delta - 1)\cos \alpha$	$(15\sin^2 \delta - 11)\sin \delta \sin \alpha$
$S_{3,1,1}$	$-\sqrt{\frac{7}{128\pi}}$	$(5\sin^2 \delta - 1)\sin \alpha$	$(15\sin^2 \delta - 11)\sin \delta \cos \alpha$
$S_{3,2,0}$	$\sqrt{\frac{35}{64\pi}}$	$\sin 2\delta \cos 2\alpha$	$(1 - 3\sin^2 \delta)\cos \delta \sin 2\alpha$
$S_{3,2,1}$	$\sqrt{\frac{35}{64\pi}}$	$-\sin 2\delta \sin 2\alpha$	$(1 - 3\sin^2 \delta)\cos \delta \cos 2\alpha$
$S_{3,3,0}$	$-\sqrt{\frac{105}{128\pi}}$	$-\cos^2 \delta \cos 3\alpha$	$\sin \delta \cos^2 \delta \sin 3\alpha$
$S_{3,3,1}$	$-\sqrt{\frac{105}{128\pi}}$	$\cos^2 \delta \sin 3\alpha$	$\sin \delta \cos^2 \delta \cos 3\alpha$

Table A5. Explicit formulae for magnetic functions $M_{nk}(\alpha, \delta)$ up to $n = 3$. For negative values of the second index, we use equation (A22).

M_{nk}	Coefficient	M_{nk}^α	M_{nk}^δ
$M_{1,0}$	$\sqrt{\frac{3}{8\pi}}$	$\cos \delta$	0
$M_{2,0}$	$\sqrt{\frac{15}{32\pi}}$	$\sin 2\delta$	0
$M_{3,0}$	$\sqrt{\frac{21}{64\pi}}$	$\cos \delta(5\sin^2 \delta - 1)$	0
$M_{1,1}$	$\sqrt{\frac{3}{16\pi}}$	$\sin \delta(\cos \alpha + i \sin \alpha)$	$-\sin \alpha + i \cos \alpha$
$M_{2,1}$	$\sqrt{\frac{5}{16\pi}}$	$-\cos 2\delta(\cos \alpha + i \sin \alpha)$	$-\sin \delta(\sin \alpha - i \cos \alpha)$
$M_{2,2}$	$\sqrt{\frac{5}{64\pi}}$	$-\sin 2\delta(\cos 2\alpha + i \sin 2\alpha)$	$2\cos \delta(\sin 2\alpha - i \cos 2\alpha)$
$M_{3,1}$	$\sqrt{\frac{7}{256\pi}}$	$\sin \delta(15\sin^2 \delta - 1)(\cos \alpha + i \sin \alpha)$	$-(5\sin^2 \delta - 1)(\sin \alpha - i \cos \alpha)$
$M_{3,2}$	$\sqrt{\frac{35}{128\pi}}$	$\cos \delta(1 - 3\sin^2 \delta)(\cos 2\alpha + i \sin 2\alpha)$	$\sin 2\delta(\sin 2\alpha - i \cos 2\alpha)$
$M_{3,3}$	$\sqrt{\frac{105}{256\pi}}$	$\sin \delta \cos^2 \delta(\cos 3\alpha + i \sin 3\alpha)$	$-\cos^2 \delta(\sin 3\alpha - i \cos 3\alpha)$

$$S_{nkp}^\alpha = \begin{cases} E_{n,k}^\alpha, & k = 0, p = 1 \\ (-1)^k \sqrt{2} \operatorname{Re} E_{n,k}^\alpha & k > 0, p = 1; \\ (-1)^k \sqrt{2} \operatorname{Im} E_{n,k}^\alpha & k > 0, p = 0 \end{cases} \quad (\text{A30})$$

$$S_{nkp}^\delta = \begin{cases} E_{n,k}^\delta, & k = 0, p = 1 \\ (-1)^k \sqrt{2} \operatorname{Re} E_{n,k}^\delta & k > 0, p = 1. \\ (-1)^k \sqrt{2} \operatorname{Im} E_{n,k}^\delta & k > 0, p = 0 \end{cases} \quad (\text{A31})$$

Table A6. Explicit formulae for electric functions $E_{nk}(\alpha, \delta)$ up to $n = 3$. For negative values of the second index, we use equation (A23).

E_{nk}	Coefficient	E_{nk}^α	E_{nk}^δ
$E_{1,0}$	$\sqrt{\frac{3}{8\pi}}$	0	$\cos \delta$
$E_{2,0}$	$\sqrt{\frac{32\pi}{15}}$	0	$\sin 2\delta$
$E_{3,0}$	$\sqrt{\frac{21}{64\pi}}$	0	$\cos \delta(5\sin^2 \delta - 1)$
$E_{1,1}$	$\sqrt{\frac{3}{16\pi}}$	$\sin \alpha - i \cos \alpha$	$\sin \delta(\cos \alpha + i \sin \alpha)$
$E_{2,1}$	$\sqrt{\frac{5}{16\pi}}$	$\sin \delta(\sin \alpha - i \cos \alpha)$	$-\cos 2\delta(\cos \alpha + i \sin \alpha)$
$E_{2,2}$	$\sqrt{\frac{5}{64\pi}}$	$-2\cos \delta(\sin 2\alpha - i \cos 2\alpha)$	$-\sin 2\delta(\cos 2\alpha + i \sin 2\alpha)$
$E_{3,1}$	$\sqrt{\frac{7}{256\pi}}$	$(5\sin^2 \delta - 1)(\sin \alpha - i \cos \alpha)$	$\sin \delta(15\sin^2 \delta - 11)(\cos \alpha + i \sin \alpha)$
$E_{3,2}$	$\sqrt{\frac{35}{128\pi}}$	$-\sin 2\delta(\sin 2\alpha - i \cos 2\alpha)$	$\cos \delta(1 - 3\sin^2 \delta)(\cos 2\alpha + i \sin 2\alpha)$
$E_{3,3}$	$\sqrt{\frac{105}{256\pi}}$	$\cos^2 \delta(\sin 3\alpha - i \cos 3\alpha)$	$\sin \delta \cos^2 \delta(\cos 3\alpha + i \sin 3\alpha)$

In vector form, these equations can be rewritten as

$$T_{nkp}(\alpha, \delta) = \begin{cases} \mathbf{M}_{n,k}(\alpha, \delta), & k = 0, p = 1 \\ (-1)^k \sqrt{2} \operatorname{Re} \mathbf{M}_{n,k}(\alpha, \delta) & k > 0, p = 1 \\ (-1)^k \sqrt{2} \operatorname{Im} \mathbf{M}_{n,k}(\alpha, \delta) & k > 0, p = 0 \end{cases} \quad (\text{A32})$$

and

$$S_{nkp}(\alpha, \delta) = \begin{cases} \mathbf{E}_{n,k}(\alpha, \delta), & k = 0, p = 1 \\ (-1)^k \sqrt{2} \operatorname{Re} \mathbf{E}_{n,k}(\alpha, \delta) & k > 0, p = 1 \\ (-1)^k \sqrt{2} \operatorname{Im} \mathbf{E}_{n,k}(\alpha, \delta) & k > 0, p = 0 \end{cases} \quad (\text{A33})$$

A3 Expansion of a real scalar function

Let us have a real function $f(\alpha, \delta)$. With the set of above-defined real scalar harmonics, we can write

$$f(\alpha, \delta) = \sum_{nkp} a_{nkp} K_{nkp}(\alpha, \delta), \quad (\text{A34})$$

where due to orthonormal basis K_{nkp} the expansion coefficients a_{nkp} are

$$a_{nkp} = \int_{\Omega} f(\alpha, \delta) K_{nkp}(\alpha, \delta) d\omega \\ = \int_0^{2\pi} d\alpha \int_{-\pi/2}^{+\pi/2} f(\alpha, \delta) K_{nkp}(\alpha, \delta) \cos \delta d\delta. \quad (\text{A35})$$

In the same way, with the system of complex scalar spherical harmonics our function can be represented as

$$f(\alpha, \delta) = \sum_{n=0}^{\infty} \sum_{k=-n}^{k=n} f_{nk} Y_{nk}(\alpha, \delta), \quad (\text{A36})$$

where

$$f_{nk} = \int_{\Omega} f(\alpha, \delta) Y_{nk}^*(\alpha, \delta) d\omega \\ = \int_0^{2\pi} d\alpha \int_{-\pi/2}^{+\pi/2} f(\alpha, \delta) Y_{nk}^*(\alpha, \delta) \cos \delta d\delta. \quad (\text{A37})$$

Taking into account equations (A8), (A35) and (A37), we obtain the relations between the expansion coefficients of one and the same function on spherical harmonics Y_{nk} and K_{nkp} :

$$f_{nk} = \begin{cases} a_{n01}, & k = 0 \\ \frac{(-1)^k}{\sqrt{2}} (a_{nk1} - i a_{nk0}), & k > 0; \\ \frac{1}{\sqrt{2}} (a_{n|k|1} + i a_{n|k|0}), & k < 0 \end{cases} \quad (\text{A38})$$

$$a_{nkp} = \begin{cases} f_{n,k}, & k = 0, p = 1 \\ (-1)^k \sqrt{2} \operatorname{Re} f_{n,k} & k > 0, p = 1 \\ (-1)^{k+1} \sqrt{2} \operatorname{Im} f_{n,k} & k > 0, p = 0 \end{cases} \quad (\text{A39})$$

A4 Expansion of a real vector function (vector field)

Now, let us have a real vector field

$$f(\alpha, \delta) = f_\alpha(\alpha, \delta) \mathbf{e}_\alpha + f_\delta(\alpha, \delta) \mathbf{e}_\delta. \quad (\text{A40})$$

Earlier, we introduced this field as expansion on real VSH equations (2), (3) and (4). Now, this expansion can be rewritten with the complex vector spherical functions

$$f(\alpha, \delta) = \sum_{n=1}^{\infty} \sum_{k=-n}^{k=n} [m_{nk} \mathbf{M}_{nk}(\alpha, \delta) + e_{nk} \mathbf{E}_{nk}(\alpha, \delta)], \quad (\text{A41})$$

where

$$\begin{aligned}
 m_{nk} &= \int_{\Omega} (f(\alpha, \delta) \mathbf{M}_{nk}^*(\alpha, \delta)) d\omega \\
 &= \int_{\Omega} (f_{\alpha}(\alpha, \delta) \mathbf{M}_{nk}^{\alpha*}(\alpha, \delta) + f_{\delta}(\alpha, \delta) \mathbf{M}_{nk}^{\delta*}(\alpha, \delta)) d\omega, \quad (\text{A42})
 \end{aligned}$$

$$\begin{aligned}
 e_{nk} &= \int_{\Omega} (f(\alpha, \delta) \mathbf{E}_{nk}^*(\alpha, \delta)) d\omega \\
 &= \int_{\Omega} (f_{\alpha}(\alpha, \delta) \mathbf{E}_{nk}^{\alpha*}(\alpha, \delta) + f_{\delta}(\alpha, \delta) \mathbf{E}_{nk}^{\delta*}(\alpha, \delta)) d\omega. \quad (\text{A43})
 \end{aligned}$$

With equations (3) and (4) and equations (A24) and (A25), we obtain the relations between coefficients \mathbf{m}_{nk} , \mathbf{e}_{nk} and t_{nkp} , s_{nkp} :

$$\mathbf{m}_{nk} = \begin{cases} t_{n01}, & k = 0 \\ \frac{(-1)^k}{\sqrt{2}} (t_{nk1} - i t_{nk0}) & k > 0; \\ \frac{1}{\sqrt{2}} (t_{n|k|1} + i t_{n|k|0}) & k < 0 \end{cases} \quad (\text{A44})$$

$$\mathbf{e}_{nk} = \begin{cases} s_{n01}, & k = 0 \\ \frac{(-1)^k}{\sqrt{2}} (s_{nk1} - i s_{nk0}) & k > 0. \\ \frac{1}{\sqrt{2}} (s_{n|k|1} + i s_{n|k|0}) & k < 0 \end{cases} \quad (\text{A45})$$

For the inverse relations, we have

$$t_{nkp} = \begin{cases} m_{n,k}, & k = 0, p = 1 \\ (-1)^k \sqrt{2} \operatorname{Re} m_{n,k} & k > 0, p = 1 \\ (-1)^{k+1} \sqrt{2} \operatorname{Im} m_{n,k} & k > 0, p = 0 \end{cases} \quad (\text{A46})$$

and

$$s_{nkp} = \begin{cases} e_{n,k}, & k = 0, p = 1 \\ (-1)^k \sqrt{2} \operatorname{Re} e_{n,k} & k > 0, p = 1. \\ (-1)^{k+1} \sqrt{2} \operatorname{Im} e_{n,k} & k > 0, p = 0 \end{cases} \quad (\text{A47})$$

APPENDIX B: MAGNITUDE EQUATION IN THE CASE OF COMPLEX VSH

As shown in the main body of our paper, the model of systematic differences depending on position and magnitude is given by equation (10). If the complex VSH are used, this equation takes the form

$$\begin{aligned}
 \Delta \mathbf{F}(\alpha, \delta, m) &= \sum_{n=1}^{\infty} \sum_{k=-n}^{k=n} \sum_r m_{nkr} \mathbf{M}_{nk}(\alpha, \delta) Q_r(m) \\
 &+ \sum_{n=1}^{\infty} \sum_{k=-n}^{k=n} \sum_r e_{nkr} \mathbf{E}_{nk}(\alpha, \delta) Q_r(m). \quad (\text{B1})
 \end{aligned}$$

In this equation, the coefficients t_{nkp} and m_{nkr} are calculated from

$$\begin{bmatrix} t_{nkp0} \\ t_{nkp1} \\ \vdots \\ t_{nkp r} \end{bmatrix} = N^{-1} \begin{bmatrix} \sum_i t_{nkp}(m_i) Q_0(m_i) \\ \sum_i t_{nkp}(m_i) Q_1(m_i) \\ \vdots \\ \sum_i t_{nkp}(m_i) Q_r(m_i) \end{bmatrix}, \quad (\text{B2})$$

$$\begin{bmatrix} m_{nk0} \\ m_{nk1} \\ \vdots \\ m_{nkr} \end{bmatrix} = N^{-1} \begin{bmatrix} \sum_i m_{nk}(m_i) Q_0(m_i) \\ \sum_i m_{nk}(m_i) Q_1(m_i) \\ \vdots \\ \sum_i m_{nk}(m_i) Q_r(m_i) \end{bmatrix}. \quad (\text{B3})$$

Here, the values m_i , $i = 0, 1, \dots, I$ are the average magnitudes at which the functions $t_{nkp}(m_i)$ and $m_{nk}(m_i)$ are determined, and N is the matrix of the normal equations formed in the LSM solution of the corresponding conditional equations:

$$N = \begin{bmatrix} \sum_i Q_0(m_i) Q_0(m_i) & \cdots & \sum_i Q_0(m_i) Q_I(m_i) \\ \vdots & & \vdots \\ \sum_i Q_I(m_i) Q_0(m_i) & \cdots & \sum_i Q_I(m_i) Q_I(m_i) \end{bmatrix}. \quad (\text{B4})$$

Obviously, the coefficients $s_{nkp}(m_i)$ and $e_{nk}(m_i)$ are determined similarly. Now, taking into account equations (A44) and (A45) we obtain relations between complex and real coefficients \mathbf{m}_{nkr} , \mathbf{e}_{nkr} and t_{nkr} , s_{nkr} :

$$\mathbf{m}_{nkr} = \begin{cases} t_{n01r}, & k = 0 \\ \frac{(-1)^k}{\sqrt{2}} (t_{nk1r} - i t_{nk0r}) & k > 0; \\ \frac{1}{\sqrt{2}} (t_{n|k|1r} + i t_{n|k|0r}) & k < 0 \end{cases} \quad (\text{B5})$$

$$\mathbf{e}_{nkr} = \begin{cases} s_{n01r}, & k = 0 \\ \frac{(-1)^k}{\sqrt{2}} (s_{nk1r} - i s_{nk0r}) & k > 0. \\ \frac{1}{\sqrt{2}} (s_{n|k|1r} + i s_{n|k|0r}) & k < 0 \end{cases} \quad (\text{B6})$$

For the inverse relations, we have

$$t_{nkr} = \begin{cases} m_{n,k,r}, & k = 0, p = 1 \\ (-1)^k \sqrt{2} \operatorname{Re} m_{n,k,r} & k > 0, p = 1 \\ (-1)^{k+1} \sqrt{2} \operatorname{Im} m_{n,k,r} & k > 0, p = 0 \end{cases} \quad (\text{B7})$$

and

$$s_{nkr} = \begin{cases} e_{n,k,r}, & k = 0, p = 1 \\ (-1)^k \sqrt{2} \operatorname{Re} e_{n,k,r} & k > 0, p = 1. \\ (-1)^{k+1} \sqrt{2} \operatorname{Im} e_{n,k,r} & k > 0, p = 0 \end{cases} \quad (\text{B8})$$